

Confined Synthesis of Zeolite Particles: micro meso porous materials

A THESIS  
SUBMITTED TO THE FACULTY OF THE GRADUATE SCHOOL  
OF THE UNIVERSITY OF MINNESOTA  
BY

James W. Wydra

IN PARTIAL FULFILLMENT OF THE REQUIREMENTS  
FOR THE DEGREE OF  
MASTER OF SCIENCE

Michael Tsapatsis

December 2010

© James W. Wydra 2010

## **Acknowledgements**

Transmission electron micrographs of samples were performed by Xueyi Zhang. Catalyst measurements were performed with the assistance of Dongxia Lui. Wei Fan provided initial training in the SAC method, and advice on other experimental design.

## **Dedication**

Anyone reading this page has to much time on their hands.

## Table of Contents

List of Figures .....	iv
Chapter 1 .....	1
1.1 Zeolite Materials .....	1
1.2 Templating Methodologies .....	2
1.3 Methods of Zeolite Growth.....	5
Chapter 2.....	6
2.1 Synthesis of Small Monodisperse Silica Particles .....	7
2.2 Small Angle X-ray Scattering.....	8
2.3 Silica Colloidal Crystal .....	11
2.4 Template Development.....	15
2.5 Synthesis of Large Silica Particles.....	19
2.6 Generation of Large Pore Template.....	21
Chapter 3.....	24
3.1 MFI Structure.....	24
3.2 Silicalite-1 Zeolites .....	25
3.3 ZSM-5 by Inclusion of Aluminum Sources in SDA Solution .....	27
3.4 ZSM-5 from Aluminum Isopropoxide.....	28
3.5 ZSM-5 Alternative Aluminum Sources .....	32
3.6 Importance of Water in Template for Silicalite-1 Synthesis .....	35
Chapter 4.....	39
4.1 BEA goal.....	39
4.2 SAC from aluminum isopropoxide SDA solution.....	41
4.3 Dry gel SAC.....	44
4.4 Templated dry gel attempts.....	45
4.5 Large carbon synthesis.....	49
Chapter 5.....	52
5.1 LTA structure.....	52
5.2 Solution synthesis of 3DOM-i LTA.....	52
5.3 MFI Growth on 3DOM-i LTA .....	59
Chapter 6.....	67
6.1 Faujasite Structure .....	67
6.2 Initial Attempt at FAU synthesis in 40 nm 3DOM template .....	68
6.3 Alternative Recipe Directed at Templated Faujasite Synthesis.....	71
6.4 Characterization of Growth Suspension .....	76
Bibliography .....	78

## List of Figures

Figure 1: Schematic of disordered carbon used as templating material: a) control of zeolite particle size <sup>14</sup> , b) inducing mesoporosity to zeolite particle <sup>15</sup> (from Schmidt and Jacobsen).....	3
Figure 2: Diagram of Autoclave with Cell for SAC.....	6
Figure 3: Scattering from 20 nm particles a) data with model prediction, b) desmeared data.....	9
Figure 4: Scattering from 40 nm particles a) data with model prediction b) desmeared data.....	10
Figure 5: PDDF functions: 20 nm (dashed line) 40 nm (solid line).....	10
Figure 6: 42 nm particles predicted SAXD in the a) FCC structure, b) BCC structure, c) HCP structure.....	13
Figure 7: SAXS plot of 40 nm silica particles with index planes.....	14
Figure 8: SAXS plot of 20 nm silica particles with index planes.....	14
Figure 9: SEM image of silica particles a) 40 nm b) 20 nm.....	15
Figure 10: 3DOM template generated from silica particles a) 37 nm b) 20 nm.....	18
Figure 11: SAXD from 3DOM templates.....	18
Figure 12: BET of Templates.....	19
Figure 13: SEM of Large Silica Particles in Colloidal Crystal.....	20
Figure 14: SEM of 3DOM carbon.....	23
Figure 15: MFI Framework Views Along [010] <sup>20</sup> .....	24
Figure 16: SEM Images of Silicalite-1 synthesized in 20 nm template.....	26
Figure 17: WAXD of silicalite-1 synthesized in 10 nm template.....	27
Figure 18: SAXD of templated silicalite-1 and template.....	27
Figure 19: WAXD of Aluminum Containing MFI Samples.....	30
Figure 20: SAXD of Aluminum Containing MFI Samples.....	31
Figure 21: SEM Images a) and b) Si/Al = 20 and c) and d) Si/Al = 40.....	31
Figure 22: SEM images of sample 1 a) and b) and sample 2 c) and d).....	34
Figure 23: WAXD of Crystalline Samples.....	35
Figure 24: SAXD of Crystalline Samples.....	35
Figure 25: SEM of Particle Morphology: a) and b) 3DOM-i MFI from Dryed Gel, c) and d) MFI from Dry Gel, and e) and f) MFI from Solution Under SAC.....	37
Figure 26: Beta Polymorph A symmetry elements <sup>19</sup> .....	40
Figure 27: Beta Polymorph B viewed along [110] <sup>22</sup> .....	40
Figure 28: Computed x-ray diffraction patterns for Beta with different amount of Polymorph A and B, where 0.9 is mostly Polymorph B <sup>22</sup> .....	41
Figure 29: Representative experimental result with commercial sample and model diffraction lines.....	43
Figure 30: SEM of representative sample result.....	43
Figure 31: SEM images from attempted synthesis of 3DOM-i BEA using water as secondary solvent.....	44
Figure 32: WAXD of Industrial Sourced BEA and Experimental Dry Gel Sample.....	45

Figure 33: WAXD of 3D0m BEA sample series .....	47
Figure 34: SEM Images from Series Samples: a) Aluminum tri-sec-butoxide with toluene mix, b) aluminum tri-sec-butoxide with TEOS mix, c) control aluminum tri-sec-butoxide with toluene mix, d) control aluminum tri-sec-butoxide with TEOS mix .....	48
Figure 35: SAXD Pattern for Template Samples .....	49
Figure 36: WAXD of Large Pore Template Sample with Industrial Sourced Material .....	50
Figure 37: SEM Images of Calcined Sample from Large Pore Carbon .....	50
Figure 38: LTA structure, drawn along the $[100]^{20}$ .....	52
Figure 39: WAXD of produced zeolite along with predicted diffraction line positions .....	54
Figure 40: SAXD of produced material.....	55
Figure 41: TEM Image of 3D0m-i LTA (image by Xueyi).....	56
Figure 42: Electron diffraction taken from the 3D0m-i LTA sample (Courtesy of Xueyi) .....	57
Figure 43: SEM images of 3D0m-i LTA .....	57
Figure 44: SEM of LTA particles from solution .....	59
Figure 45: WAXD of synthesized samples.....	60
Figure 46: SAXD of synthesized samples .....	60
Figure 47: BET isotherms before and after SAC growth of 3:100 material .....	60
Figure 48: a and b 3:100 with c and d 10:100.....	61
Figure 49: a) and b) 3D0m-i LTA with 3:100 mg ratio, c) and d) 3D0m-i LTA with 10:100 mg ratio (Courtesy of Xueyi).....	62
Figure 50: WAXD for samples and base material .....	64
Figure 51: SAXD of C3 Samples.....	64
Figure 52: a and b at 135 °C and c and d at 70 °C .....	65
Figure 53: Control samples of C3 Solution: a and b from 135 °C and c and d from 70 °C .....	66
Figure 54: Faujasite framework viewed down the $[111]^{20}$ .....	67
Figure 55: SEM images of 3D0m-i FAU synthesized along with FAU large crystals. ....	69
Figure 56: WAXD of 3D0m-i FAU .....	70
Figure 57: SAXD of 3D0m-i FAU .....	70
Figure 58: WAXD of Sample after Second and Third Cycles of Growth .....	73
Figure 59: SAXD after Cycle 3 of Growth .....	73
Figure 60: TEM Image of Material after Cycle 3 (Image by Xueyi).....	74
Figure 61: SEM Images of Material .....	74
Figure 62: WAXD of Material after Calcination and 4 Growth Cycles .....	75
Figure 63: SEM Images of Material .....	76
Figure 64: SEM Images of Colloidal Crystals from 3D0m-i FAU growth .....	77
Figure 65: WAXD of Crystals from 3D0m-i FAU Growth with LTA Model Lines....	77

## Chapter 1

### Zeolites and Micro Meso Porous Materials

#### 1.1 Zeolite Materials

Zeolites are crystalline aluminosilicate materials, with highly order micropore structures which have been sought after for many applications. Zeolite materials have been applied to many traditional operations, such as catalysts, absorbants, and ion exchange materials<sup>1</sup>. Recent research into zeolites has also suggested potential applications in chemical sensors<sup>2</sup>, low k-dielectrics<sup>3</sup>, contrast agents for magnetic resonance imaging<sup>4</sup>, and photocatalytic materials<sup>5</sup>. In order to advance the development of zeolites for these applications, control over the particle size is a desired synthetic tool, as well as the ability to synthesize particles with mesopores while retaining the zeolite.

Zeolites are composed of a network of  $\text{AlO}_4^{-1}$  and  $\text{SiO}_4$  tetrahedra linked together in various structures<sup>1</sup>. The tetrahedra of aluminum and silicon link together to form secondary building units which combine together to form over 200 different zeolite structures. Rings of 6, 8, 9, 10, and 12 tetrahedra result in the microporous structure of zeolites. The pore diameter in the zeolite structure typically range from 3 to 8 Å depending on the number of tetrahedral atoms which form the ring channel within the structure. Within these pores are water molecules and cations which balance the charge within the framework. Pores are classified into three regimes: under 2 nm are considered micropores, those in the range of 2 nm to 50 nm are classified as mesopores, and those above 50 nm are macropores<sup>6</sup>. Mesopores are a desired characteristic to reduce diffusion

limitations within zeolite structure while still maintaining the selectivity of the micropores in the structure.

In recent years there has been a substantial effort in developing zeolite crystals with particle sizes less than 200 nm<sup>7</sup> and forming crystals with mesopores<sup>8,9,10</sup>. The change in particle size from the micron scale to the nanometer scale will influence the performance of zeolites used for separation and catalytic applications. Decreasing particle size increases the surface area and therefore the surface activity of the particle as well as reducing the diffusion path length, which will improve catalytic performance. Imparting crystals with mesopores has the similar effect of reducing diffusional path lengths of molecules through the crystal structure leading to enhanced performance.

## 1.2 Templating Methodologies

Synthesizing mesoporous materials with a zeolitic framework has been the focus of a substantial research effort and has resulted in four basic strategies. Previous approaches have attempted to utilize surfactants in zeolite synthesis solutions; however the result tends to be a mixture of zeolite crystals and amorphous mesoporous material<sup>11</sup>. Alternatively, zeolite seed crystals were mixed with surfactants in an attempt to assemble a mesoporous material, this resulted in increased acid catalytic activity; however the framework did not possess zeolite crystallinity<sup>11,12</sup>. A third approach towards mesoporosity utilizes an organosilane surfactant to direct the formation of mesopores within the zeolite structure<sup>13</sup>. This method results in mesoporous zeolite particles, built from randomly oriented nanocrystals, with high crystallinity and reduced diffusional limitations<sup>11,13</sup>. This method has been used to generate the MFI structure with

mesoporosity, which has demonstrated enhanced catalytic activity compared to conventional MFI crystals<sup>11,13</sup>.

The fourth approach, and method of interest for this work, has been to utilize ridged templates to control mesoporosity. Through the use of a carbon template, the size of zeolite particles can be controlled and the particles can be imparted with mesoporosity<sup>8,9,10,14,15</sup>. Zeolite crystals can be formed within the confined space generated during the disordered packing of carbon particles<sup>14</sup>. Alternatively, large zeolite crystals can be grown around multiple carbon particles which upon combustion generate mesopores in the zeolite particle<sup>15</sup>. Below, figure 1 represents schematically how these two types of templating would occur.

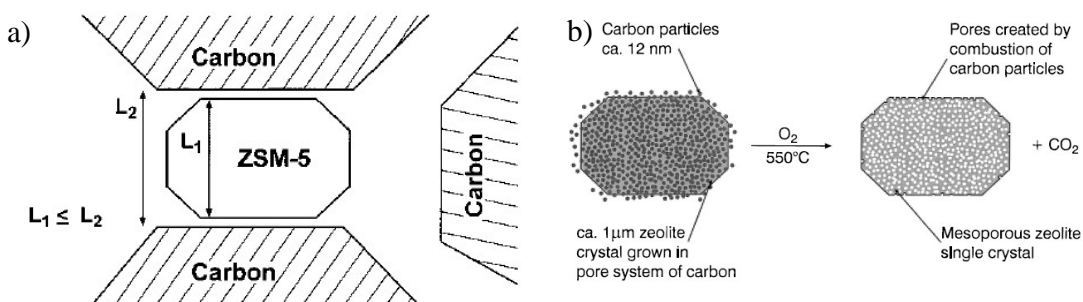


Figure 1: Schematic of disordered carbon used as templating material: a) control of zeolite particle size<sup>14</sup>, b) inducing mesoporosity to zeolite particle<sup>15</sup> (from Schmidt and Jacobsen)

Recently there has been a shift from a disordered carbon template, to one possessing long range ordering. Three-dimensionally ordered macroporous (3DOM) carbon template has been utilized to synthesize ZSM-5, MFI framework, zeolite material<sup>8</sup>. 3DOM carbon has a pore size on the macroscopic scale, approximately 200 nm. ZSM-5

was synthesized in this template through a solution growth method, in which the template is immersed in the growth solution, heated for two days, then washed with water. This procedure was repeated multiple times to fill the template pores with zeolite crystals<sup>8</sup>.

A carbon template with smaller pores, on the mesoscale, has been recently synthesized in the Tsapatsis lab, and utilized to grow ZSM-5 particles<sup>9</sup>. The carbon template has a tunable pore size between 10-40 nm, and termed three-dimensionally ordered mesoporous (3DOM) carbon. ZSM-5 particles were synthesized within the 3DOM template using a steam assisted growth method, as opposed to a solution growth method observed in 3DOM. For this technique, the carbon template was impregnated to incipient wetness with the synthesis solution. The template is heated in a saturated water vapor which supports the growth of particles. During steam assisted growth particles nucleate and grow within the template pores, forming ZSM-5 particles.<sup>9</sup>

Zeolite structures other than MFI have yet to be produced with in these ordered carbon templates. Other zeolites formed within these highly ordered templates are desired for potential membrane and catalytic applications. Two zeolites structures of particular interest are the beta and faujasite structure. Both the beta and faujasite structures are utilized as catalysts for various reactions. Synthesizing both beta and faujasite with mesoporosity imparted by the carbon template is desired as a potential method to improve catalytic activity through reduced diffusional length and decrease deactivation from coking.

### 1.3 Methods of Zeolite Growth

Traditionally zeolite synthesis is performed by a hydrothermal growth method, where a growth solution or gel is heated to elevated temperatures. Hydrothermal treatment involves heating the reaction mixture dispersed in water to elevated temperatures, where nucleation and growth of the zeolite phase occurs from the precursor materials present. This can occur at a variety of temperature, from low temperature around room temperature up to highly elevated temperature around 200 °C. The temperature used is highly dependent on the composition of the growth media and the desired zeolite phase.

More recently, new methods like vapor phase transport (VPT) and steam assisted crystallization (SAC) have been developed and used to generate zeolite particles. VPT relies on utilizing a volatile structure directing agent that is separated from the dried silica and alumina precursors. Upon heating, the volatile structure directing agent and steam interact with the silica and alumina in the vapor phase, causing the evolution of a zeolite phase within the dry powder of silica and alumina. This method was described for the synthesis of ZSM-5 by Xu<sup>16</sup>, where the volatile SDA ethylenediamine (EDA) was used to transform a dry gel of alumina and silica into zeolite at temperatures between 180 to 200 °C. The ethylenediamine and water evaporate upon heating, transforming the amorphous solid phase into a crystalline zeolite phase. SAC is very similar to VPT except that the solid phase is mixed with a non-volatile SDA. Here water, external to the dry gel, when vaporized acts to transform the amorphous dry gel into a crystalline zeolite phase.

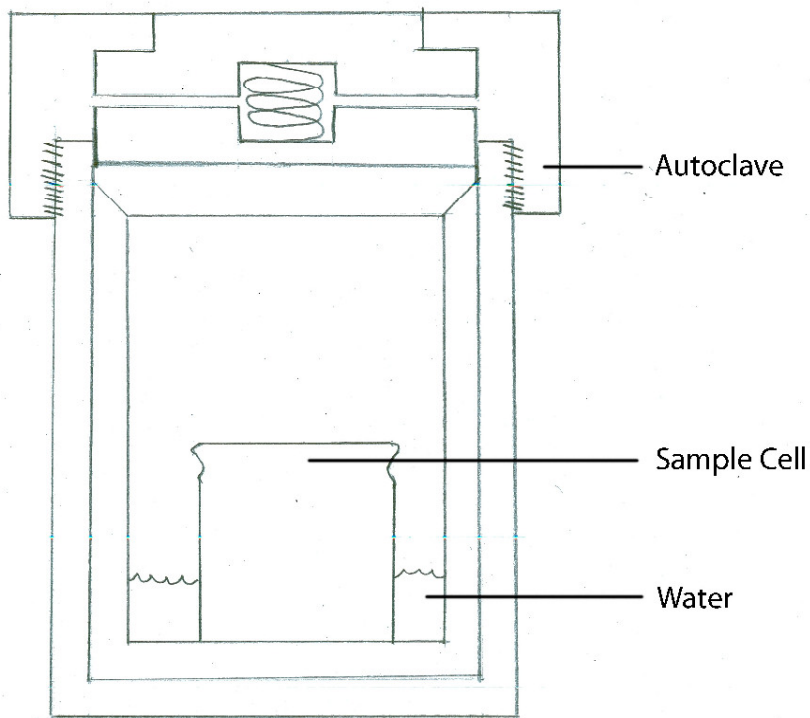


Figure 2: Diagram of Autoclave with Cell for SAC

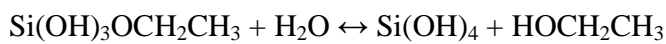
Figure x above diagrams how the sample vessel is set up for SAC or VPT. In each case, the dry gel is located inside the sample cell. The sample cell separates the dry gel from the exterior liquid that will produce the saturated steam environment needed for the transformation of amorphous dry gel into zeolite material. The sample cell can be made of glass, ceramic, or Teflon, any material that has the appropriate stability can be utilized to isolate the dry gel from the liquid.

## Chapter 2

Synthesis and Characterization of Silica Nanoparticles for Colloidal Crystal Formation

## 2.1 Synthesis of Small Monodisperse Silica Particles

Silica particles can be synthesized from the hydrolysis of organic silica sources such as tetraethyl orthosilicate (TEOS). TEOS hydrolyzes in the presence of water, typically acid or base catalyzed, to generate ethanol and silica.



By including L-lysine in the mixture, a basic amino acid, the rate of hydrolysis can be controlled. By controlling the rate of hydrolysis, monodisperse silica particles can be generated<sup>17</sup>.

The size of the silica particles can be manipulated by altering the temperature of the hydrolysis reaction and the stirring rate of the reaction mixture. Higher temperatures can be utilized to increase the particle size generated. Faster stirring rates can be used to decrease the size of the synthesized particles.

20 nm particles can be generated by with a mixture of silica, L-lysine, and water with a mole ratio of 61 TEOS: 1.19 L-lysine: 9500 water (15.6 g TEOS, 0.213 g L-lysine, 210 g water). The reaction mixture is heated to 90 °C in an oil bath and mixed at 500 rpm for 24 hours. After 24 hours, the mixture is cooled to a handle able temperature and poured into a crystallization dish to evaporate the solvent. The evaporation of water and ethanol leads to the formation of a colloidal crystal composed of 20 nm particles.

Larger diameter monodisperse particles can be generated with a seeded growth method. First the recipe from generating 20 nm particles is followed. After the reaction reaches completion however, instead of evaporating the solvent, additional TEOS is added to enlarge the existing silica particles. This seeded growth method is typically utilized to generate particles with a diameter of 40 nm. 40 nm particles are formed through two seeded growth steps, each consisting of an additional addition of 31.2 g of TEOS to the reaction mixture, then reheating to 90 °C for 24 hours, mixed at 500 rpm. After the two seeded growth steps, the particles can be precipitated into a colloidal crystal by removal of the water and ethanol.

The silica particles in solution can be characterized by small angle x-ray scattering to determine particle size, as well as particle density.

## 2.2 Small Angle X-ray Scattering

After synthesis, particles can be analyzed in growth solution with small angle x-ray scattering (SAXS). The 40 nm particle recipe requires dilution with DI water due to strong the strong signal produced from the concentrated solution of particles. Scattering analysis was performed on the SAXSess instrument at the characterization facility which operates with a partial beam stop and records data on an imaging plate. Scattering from the particles in solution were subtracted from scattering background due to water.

The particle scattering was modeled with PCG software package. The raw data was binned into  $q$  ranges of 0.01 to 0.5, 0.5 to 1, 1 to 2, and 2 to 8 with a compression of 1, 2, 4, and 8 respectively. The spheres were then modeled as monodisperse, with smearing from slit length and width of the line collimator. The pair distance distribution function

(PDDF,  $P(r)$ ) could then be determined for each particle size. The data was handled by the following equations:

$$q = \frac{4\pi n}{\lambda} \cdot \sin(\theta)$$

$$I(q) = 4\pi \int_0^{\infty} P(r) \frac{\sin(qr)}{qr} dr$$

$$P(r) = r^2 \left\langle \int_V \Delta\zeta(r_1) \cdot \Delta\zeta(r_1 - r) dr \right\rangle$$

$$P_{sphere}(q, r) = \left[ \frac{3[\sin(q \cdot r) - q \cdot r \cos(q \cdot r)]}{(q \cdot r)^3} \right]^2$$

Where the PDDF was handled with an indirect Fourier transform for limited  $q$  range.

The scattering data was plotted with the models predicted intensity against  $q$  in  $\text{nm}^{-1}$  for 20 and 40 nm particles. The PDDF for each particle was plotted as a function of  $r$  in nm, which can be used to determine the experimental particle size.

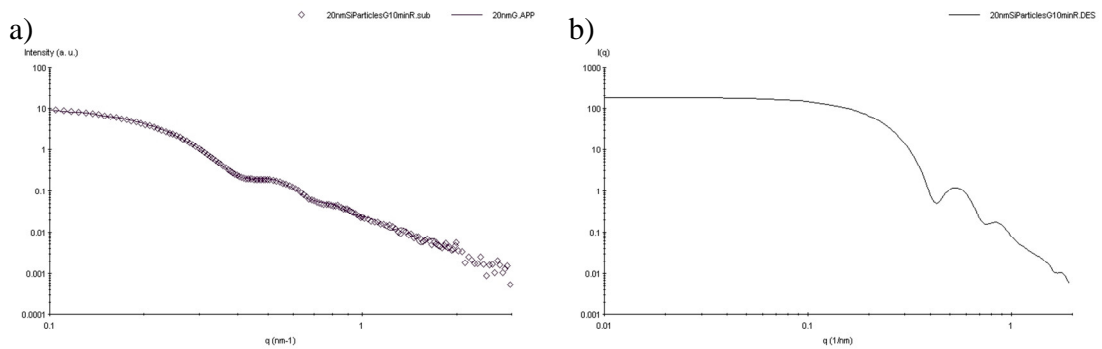


Figure 3: Scattering from 20 nm particles a) data with model prediction, b) desmeared data

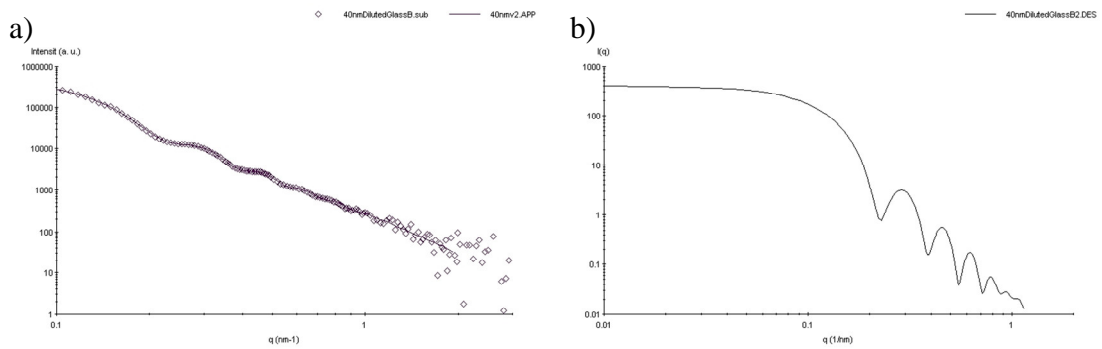


Figure 4: Scattering from 40 nm particles a) data with model prediction b) desmeared data

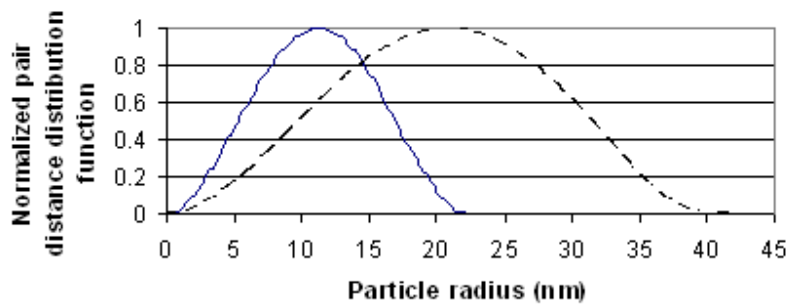


Figure 5: PDDF functions: 20 nm (dashed line) 40 nm (solid line)

From the scattering data, it can be determined that the particles are close to 22 nm and 42 nm in diameter and monodisperse in size. 22 nm and 42 nm are the standard sizes used for template development. The size of the particles can be controlled to give intermediate sizes as well as smaller particles by altering the synthesis conditions.

Additionally, the number density of particles in solution can be calculated. The number density of 20 nm particles is calculated to be  $2.18 \cdot 10^{15}$  and the number density of 40 nm particles is calculated to be  $1.47 \cdot 10^{15}$ . The number density was determined by solving the following two equations:

$$\frac{4\pi}{3}r^3 = v_{SiO_2} \left( \frac{C_{SiO_2}}{n} \right) + v_{H_2O} y_{H_2O}$$

$$I^{abs}(q=0) = n \left( \frac{4\pi}{3}r^3 \right)^2 (\Delta SLD)^2 \left( \frac{C_{SiO_2}/n}{C_{SiO_2}/n + y_{H_2O}} \right)^2$$

Where  $n$  is the number of particles and  $C_{SiO_2}$  is the concentration of silica particles.  $v_{SiO_2}$  and  $v_{H_2O}$  are the volume per mole of water and silica. The concentration of silica particles is determined by the total amount of silica added and the monomer solubility of silica in solution based on pH of the system.

$$[SiO_2]_{total} = [SiO_2]_{monomer} + [SiO_2]_{particle}$$

$$[SiO_2]_{CAC} = 24.147[OH^-] + 0.016 \sim 0.016$$

$$contrast = [x_{SiO_2} SLD_{SiO_2} + (1 - x_{SiO_2}) SLD_{H_2O}] - SLD_{Background}$$

The scattering length density for water and silica were taken from the publication of Rimer<sup>18</sup>, which discusses the equations used in this method. By taking the experimentally determined  $I^{abs}(q=0)$  and following these equations  $n$ , the number of particles per volume, can be determined.

### 2.3 Silica Colloidal Crystal

The formation of colloidal crystal takes place as the solvent is removed from the silica particles in a crystallization dish. The dispersion of particles is heated to 70 °C in a crystallization dish to remove the water and ethanol, leaving behind the silica particles packed in an ordered structure.

The spheres will form a close packed structure, being either body centered, face centered, hexagonal, a combination of these structures, or a random close packed structure. From small angle x-ray diffraction (SAXD), it is known that the particles form an ordered structure. Based on Bragg's Law and the particle size, diffraction peaks for each structure can be calculated.

$$n \cdot \lambda = 2 \cdot d \cdot \sin(\theta)$$

$$d_{cubic} = \frac{a}{\sqrt{h^2 + k^2 + l^2}}$$

$$d_{hcp} = \frac{\sqrt{3}}{2} \frac{a}{\sqrt{h^2 + h \cdot k + k^2}} + \frac{1.633 \cdot a}{l}$$

$$\frac{2\pi}{q} = d$$

Given the spherical particles are in contact with one another, the radius of the particle can be related to the lattice parameter directly. For a face centered cubic structure  $a$  is equal to  $2\sqrt{2}r$ , a body centered cubic structure  $a$  is equal to  $\frac{4}{\sqrt{3}}r$ , and for the hexagonal structure  $a$  is equal to  $2r$ . Given these structural relationships, and the distance equations, 5 and 6, the diffraction conditions can be determined. Following the selection rules for each structure, and estimating the relative intensities from similar metal structures, the SAXD patterns can be calculated.

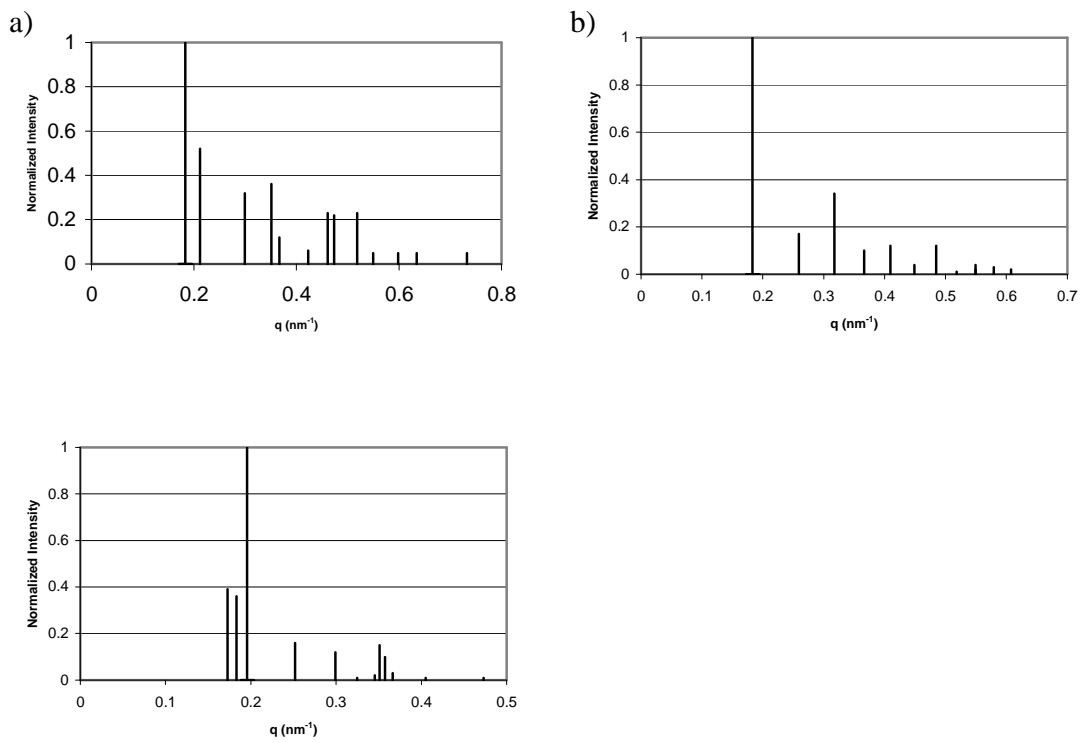


Figure 6: 42 nm particles predicted SAXD in the a) FCC structure, b) BCC structure, c) HCP structure

Experimental SAXD patterns can be obtained from the colloidal crystal following removal of the solvent. Experimental data is plotted against the log of normalized intensity, to make higher order peaks more observable.

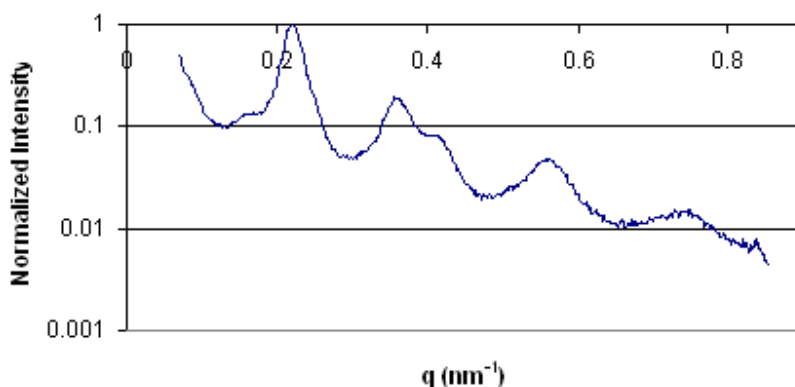


Figure 7: SAXS plot of 40 nm silica particles with index planes

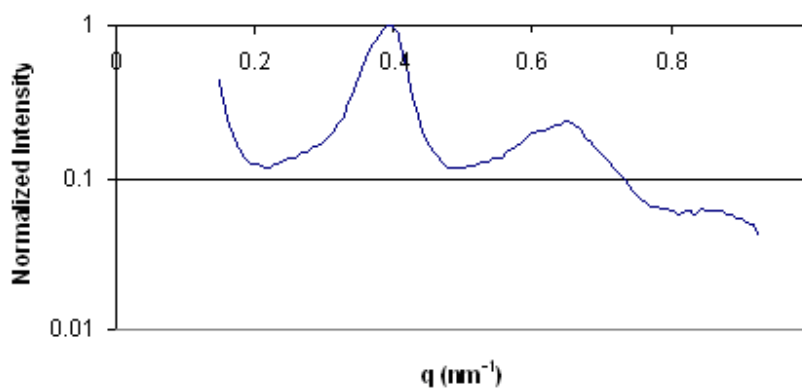


Figure 8: SAXS plot of 20 nm silica particles with index planes

The SAXD patterns do not show a definitive matching to any of the close packed structures expected. It is clear there is a high degree of ordering to the colloidal crystal, however trying to index the peaks to FCC, BCC, or HCP is not very clear. The FCC structure represents the most alignment of predicted diffraction peaks to the experimentally observed diffraction, however this is far from perfect agreement. It is possible that the colloidal crystal formed is in fact a combination of FCC and BCC ordering with wide peak areas.

In addition to x-ray analysis of these silica particles, scanning electron microscopy (SEM) can be utilized for analysis. SEM confirms the spherical shape of the silica particles. It also displays the ordered structure of the colloidal crystal, but does not give much insight into its actual structure. SEM can also be used to confirm the particle size of the synthesized silica particles.

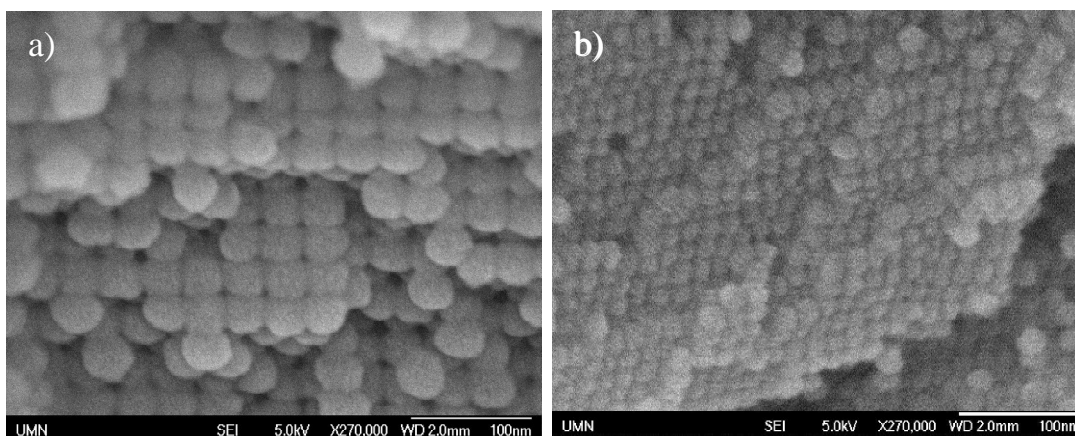


Figure 9: SEM image of silica particles a) 40 nm b) 20 nm.

## 2.4 Template Development

Following analysis of the colloidal crystal, the silica particles need to be calcined to remove the surface lysine. Calcination also results in the neighboring particles fusing together at high temperatures. The calcination is performed at 550 °C in air.

After the particles are calcined, the template is formed around the particles. A mixture of furfuryl alcohol and oxalic acid is formed at a 200:1 weight ratio. Oxalic acid acts to catalyze the polymerization of furfuryl alcohol. After the oxalic acid has been dispersed in furfuryl alcohol with the aid of sonication, the mixture can be added to the colloidal crystal silica. The mixture is added to the colloidal crystal with a slight excess, to ensure complete impregnation of the monomer mixture. The mixture is allowed to sit on the

colloidal crystal with some hand mixing for 5 minutes. After approximately 5 minutes the excess liquid is removed from the colloidal crystal. Filter paper is used to remove the excess liquid from the solid particles. The particles are then transferred to a plastic bottle with Teflon tape, which aids in sealing the vessel. The bottle is sealed and then placed in the oven at 70 °C for 2 days, so the furfuryl alcohol can polymerize around the silica particles.

After the 2 days, the polymer and particles can be removed from the oven. At this point the solid is dark brown to black color, indicating completion of polymerization. The solid is transferred to a quartz tube reactor system. Quartz reactor is used in the next set due to the high temperature that is needed for carbonization. The reactor is designed to allow an inert gas to flow over the sample while the sample is placed down into a furnace for high temperature treatment. The furnace is programmed to heat the sample as follows: heat to 200 °C over 2 hours, hold at 200 °C for 2 hours, heat to 850 °C over 7 hours, hold at 850 °C for 4 hours, then cool naturally. This temperature program was performed under a nitrogen or helium environment, although any inert gas that prevents the combustion reaction will work.

After the carbonization reaction, a black solid is produced. This black solid needs to be etched of the silica particles to leave only the carbon template. Etching of the silica is done by placing the solid in a Teflon liner, to which 6 M potassium hydroxide (KOH) solution is added. The liner is then placed into an autoclave, where the KOH solution is heated to 180 °C for 2 days. The solid is then removed from the KOH solution by vacuum filtering on a Whatman 542 filter pad, and washed with DI water. The solid is then

collected and placed back into the Teflon liner. Fresh KOH solution is added to the liner and the liner is sealed in an autoclave for another 2 days of 180 °C etching. The carbon is once again isolated from the KOH solution on a Whatman 542 filter pad, and washed with additional water.

This time the carbon is collected in a 1 L bottle. The bottle is then filled with DI water, mixed and placed in an oven to warm to 70 ° for 3 hours. This is done to wash the carbon to remove any residual potassium that may be present. After warming for 3 hours, the carbon is collected and the wash water is disposed of. The process of washing with DI water is repeated until the wash water has an essentially neutral pH. This typically takes 7 washing cycles. The carbon can be isolated from the wash water by filtration, or decanting of the wash water off the carbon solid can also be performed. After completing the washings, the carbon is dried.

The carbon can be characterized with SEM and SAXD. Like the particles, small angle x-ray diffraction can be used to observe the ordering within the template. The diffraction intensity of the template is lower than that of the silica particles. Similarly, SEM is used to confirm the ordered pattern is retained during carbonization and etching. SEM is also useful to check that most of the silica was indeed etched out of the carbon.

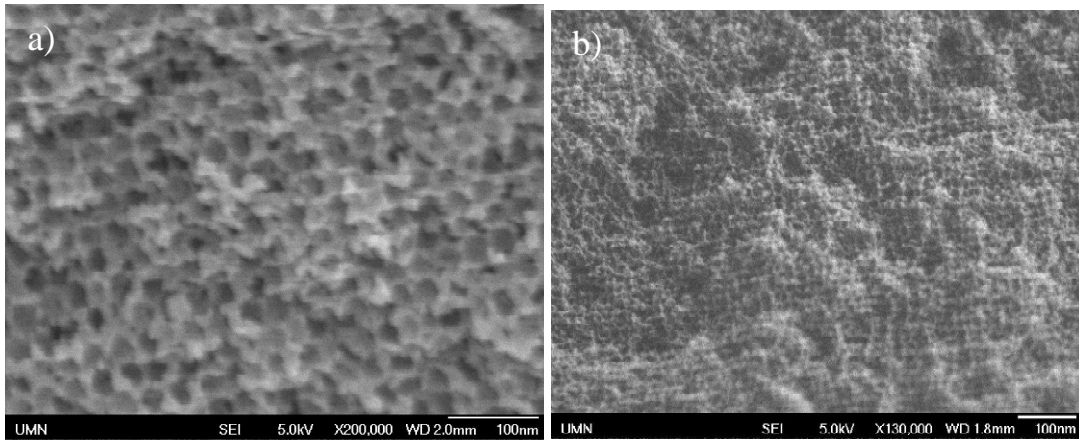


Figure 10: 3D porous template generated from silica particles a) 37 nm b) 20 nm

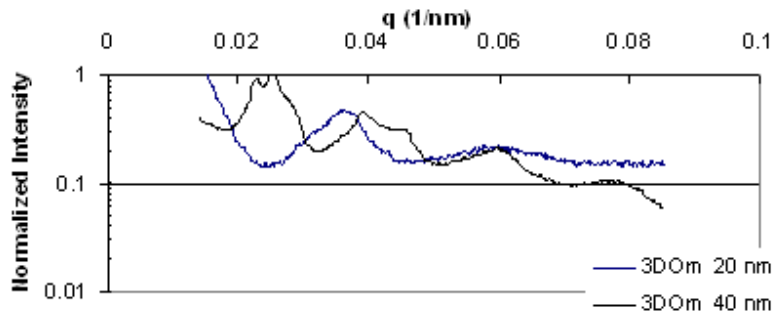
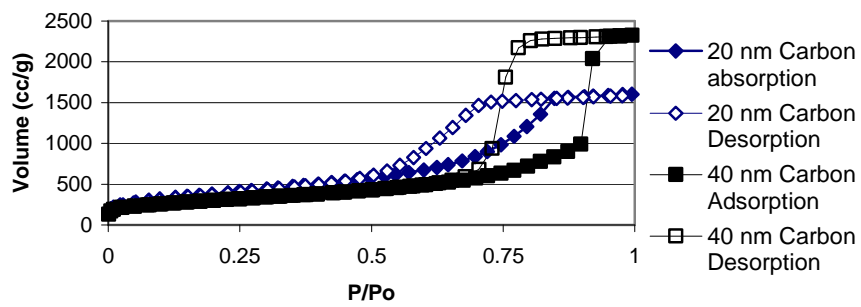


Figure 11: SAXD from 3D porous templates



## Figure 12: BET of Templates

From the included characterization data, it can be seen that the template does form an inverse of the silica particles. This template will be used in future experiments to control the growth of zeolite particles, and induce mesoporosity into the zeolite particles.

### 2.5 Synthesis of Large Silica Particles

An alternative method to synthesizing monodisperse silica particles with larger diameters was discovered and published by Stober<sup>19</sup>. This method does not use L-lysine to control particle formation, but relies on ammonium hydroxide for the rapid nucleation of particles and then the slower transformation into a monodisperse system. The published method investigates how the particle size can be tuned by controlling concentration of ammonium hydroxide, TEOS, and water. Different alcohols can also be used to tune the size of the synthesized particles.

In order to generate silica particles from this recipe ethanol, water, and ammonium hydroxide (35 wt%) were measured out volumetrically into a bottle or round bottom flask with a stir bar. These ingredients were mixed for approximately 10 minutes. Tetraethyl orthosilicate was then measured out volumetrically and poured into the vessel while mixing. The vessel was sealed and allowed to sit at room temperature while undergoing vigorous mixing for 24 hours. The recipe used: 13.9 mL ammonium hydroxide, 3.6 mL water, 100 mL ethanol, and 4.48 mL TEOS.

After mixing for 24 hours, the suspension of particles was poured into centrifuge tubes. The tubes were then balanced and centrifuged to separate the particles from the ethanol solution. The ethanol solution was then poured off the tubes. Fresh water was

added to the tubes, and the particles were re-dispersed by shaking. The particles were then isolated again by centrifugation. The wash water was then poured off again. The particles were again re-dispersed in water, this time with the aid of sonication as well as mixing. The particles could then be isolated by centrifugation. This time the particles were re-dispersed in a minimal amount of water, with the aid of sonication. This concentrated suspension was poured into a crystallization dish, or a weighing glass depending on the amount of particles generated. The water was then evaporated at 70 °C, to produce a colloidal crystal of large silica particles.

The colloidal crystal can be characterized optically by the refraction of visible light and by SEM. The particles can also be characterized in solution by dynamic light scattering.

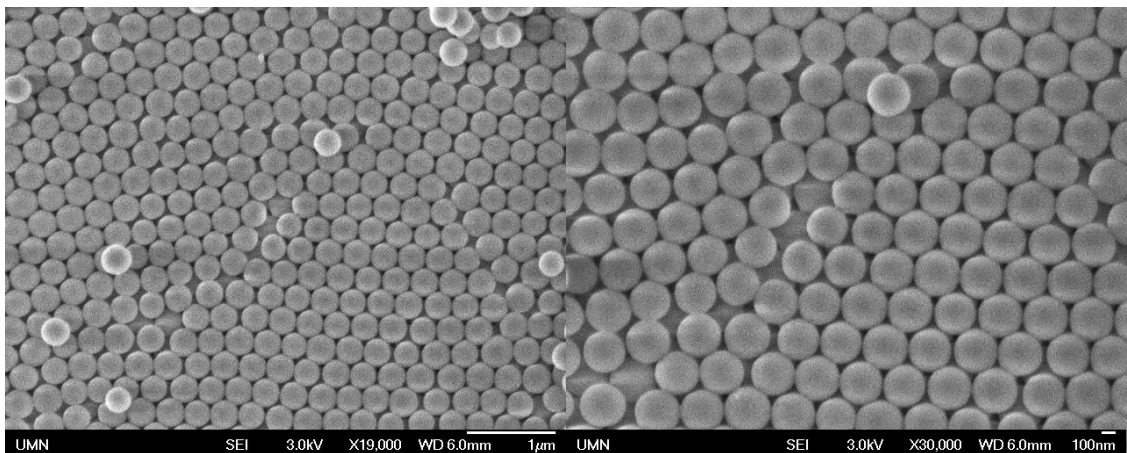


Figure 13: SEM of Large Silica Particles in Colloidal Crystal

From the SEM images, the particles have a size of approximately 300 nm and are close packed. DLS can be utilized to confirm this particle size and suggest a high degree of monodispersity.

## 2.6 Generation of Large Pore Template

From the large diameter silica particles, a large pore carbon template can be synthesized using a similar procedure. Furfuryl alcohol and oxalic acid are used, in a 200 to 1 ratio, to form a polymer around the colloidal crystal. The mixture of furfuryl alcohol and oxalic acid are added to calcined large silica particles. The liquid solution is mixed with the particles given approximately 10 minutes for the solution to reach all the mesopores between the silica particles. Excess solution is removed from the solid using filter paper to absorb the furfuryl alcohol solution. The solid looks like a wet white solid material as it is placed in a small bottle for polymerization to occur in. The sealed bottle is heated to 70 °C for two days where polymerization occurs.

After the two days, the collected solid is placed in a quartz reactor for carbonization of the polymer. The reactor is designed to allow an inert gas to flow over the sample while the sample is placed down into a furnace for high temperature treatment. The furnace is programmed to heat the sample as follows: heat to 200 °C over 2 hours, hold at 200 °C for 2 hours, heat to 850 °C over 7 hours, hold at 850 °C for 4 hours, then cool naturally. This temperature program was performed under a nitrogen or helium environment, although any inert gas that prevents the combustion reaction will work.

After the carbonization reaction, a black solid is produced. This black solid needs to be etched of the silica particles to leave only the carbon template. Etching of the silica is done by placing the solid in a Teflon liner, to which 6 M potassium hydroxide (KOH) solution is added. The liner is then placed into an autoclave, where the KOH solution is heated to 180 °C for 2 days. The solid is then removed from the KOH solution by vacuum

filtering on a Whatman 542 filter pad, and washed with DI water. The solid is then collected and placed back into the Teflon liner. Fresh KOH solution is added to the liner and the liner is sealed in an autoclave for another 2 days of 180 °C etching. The carbon is once again isolated from the KOH solution on a Watman 542 filter pad, and washed with additional water. Due to the large amount of silica present, a third etch is performed to ensure all the silica is removed from the template. After the third etch the solid is collected for washing with DI water.

The carbon is collected in a 1 L bottle. The bottle is then filled with DI water, mixed and placed in an oven to warm to 70 ° for 3 hours. This is done to wash the carbon to remove any residual potassium that may be present. After warming for 3 hours, the carbon is collected and the wash water is disposed of. The process of washing with DI water is repeated until the wash water has an essentially neutral pH. The carbon can be isolated from the wash water by filtration, or decanting of the wash water off the carbon solid can also be performed. After completing the washings, of the carbon is dried.

After the carbon is dried, it can be characterized by SEM. SEM shows that the inverse opal shape is developed based on the colloidal crystal silica particles. This type of carbon is termed three dimensionally ordered macro porous, 3DOM, carbon.

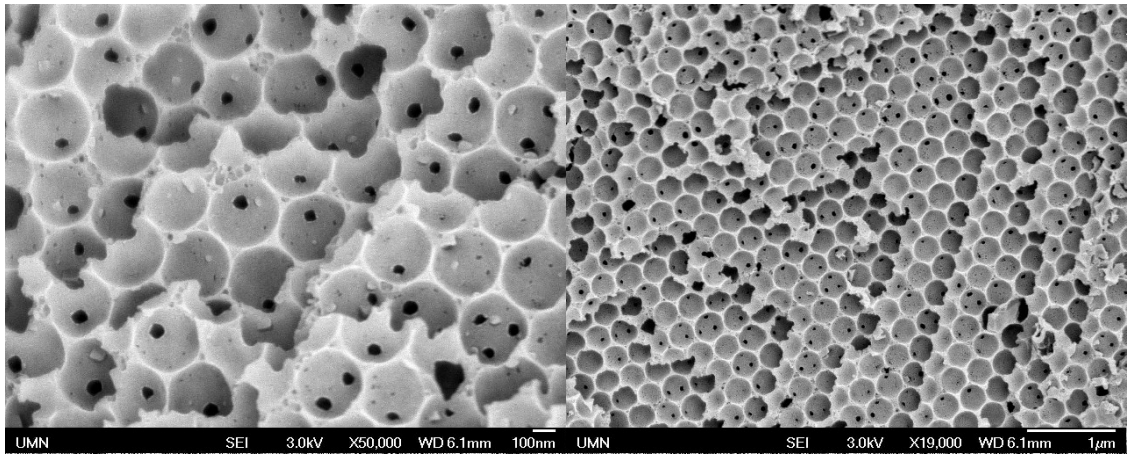


Figure 14: SEM of 3DOM carbon

## Chapter 3

### Synthesis of 3D Om templated MFI Structured Zeolites for Catalytic Reaction

#### 3.1 MFI Structure

The MFI structure is an aluminosilicate structure with 10 member rings which compose channels in the a and b directions. The channels in the MFI structure have a pore diameter of 5.3 nm in the b direction and 5.1 nm in the a direction<sup>20</sup>. The formula for the MFI structure is given by  $\text{Na}_n^+(\text{H}_2\text{O})_{16}\text{Al}_n\text{Si}_{96-n}\text{O}_{192}$  where sodium is used as the counter ion for the frame work aluminum.

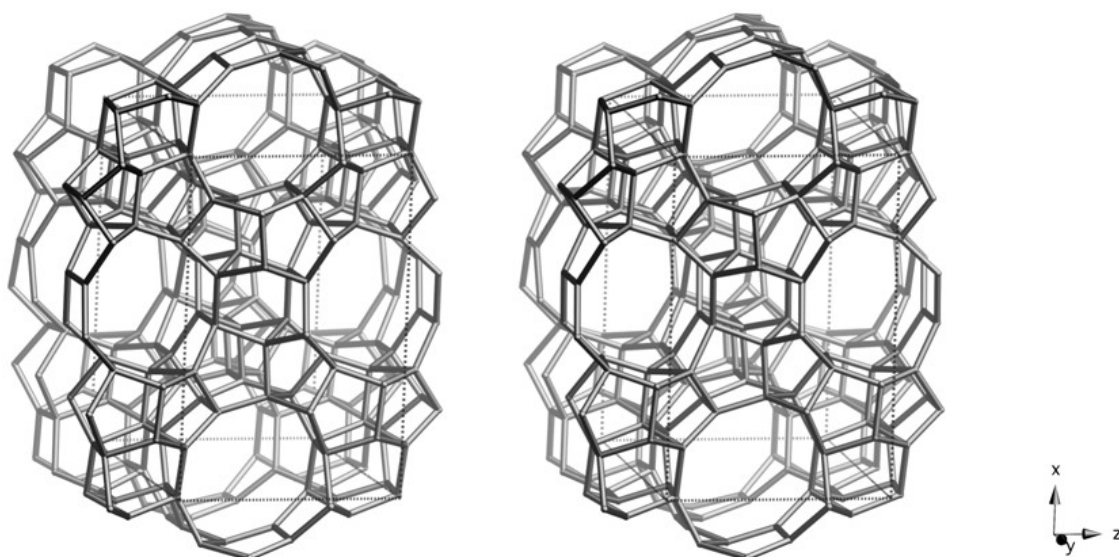


Figure 15: MFI Framework Views Along [010]<sup>20</sup>

The MFI is one of the easiest zeolite structures to generate, capable of being synthesized in an all silica form, Silicalite-1, and a wide range of Si/Al ratios.<sup>21</sup>

### 3.2 Silicalite-1 Zeolites

Steam assisted crystallization has been shown as a successful method to grow silicalite-1 zeolite particles within 3DOM carbon. In order to perform this method, 3DOM carbon is dried overnight at temperatures above 100 °C. This 3DOM carbon will be the template which the zeolite particles are grown within. By varying the template pore size (size of colloidal particles used to generate the template) the size of the zeolite can be manipulated.

The structure directing agent (SDA) solution is made from tetrapropylammonium hydroxide (40 wt%) (TPAOH), water, sodium hydroxide, and ethanol (EtOH). The 4 reagents are mixed together before adding to the carbon template. The silica is provided to the reaction mixture in an organic form as tetraethylorthosilicate (TEOS). The final reaction mol ratio of components is 18 TPAOH:0.3 NaOH:390 water:180 EtOH:50 SiO<sub>2</sub>. The ethanol is removed through evaporation before the addition of TEOS.

The SDA solution is formed by mixing 4.576 g of TPAOH (40 wt%), 0.021 g of 10 m NaOH solution, 0.753 g of water, and 4.146 g of EtOH (200 proof). The dried carbon is massed into a vial, where the typical mass is 0.15 g of carbon. To the carbon, the SDA solution is added volumetrically with a micro-pipette. The volume of addition is dependent on the pore size of carbon utilized. The vial is subsequently massed, and then placed in the fume hood. After the ethanol has evaporated, based on sample mass, the TEOS can be added to the carbon. TEOS, is also added volumetrically to the sample. The vial is then placed in a Teflon liner which contains approximately 3 g of water. The vial is then sealed in an autoclave. The autoclave is allowed to sit at room temperature

for at least 3 hours for the sample to age. Longer aging times can be performed. The sample then undergoes SAC in autogenerated atmospheres.

Two SAC recipes have been demonstrated to generate silicalite-1 particles. The sample can be heated to 180 °C for 1 day, followed by rapid quenching in water. Alternatively, the sample can be heated to 135 °C for 3 days, followed by rapid quenching in water. After synthesis, the carbon can be removed by calcination in air at 550 °C. The resulting product can be analyzed with WAXD, SAXD, and SEM.

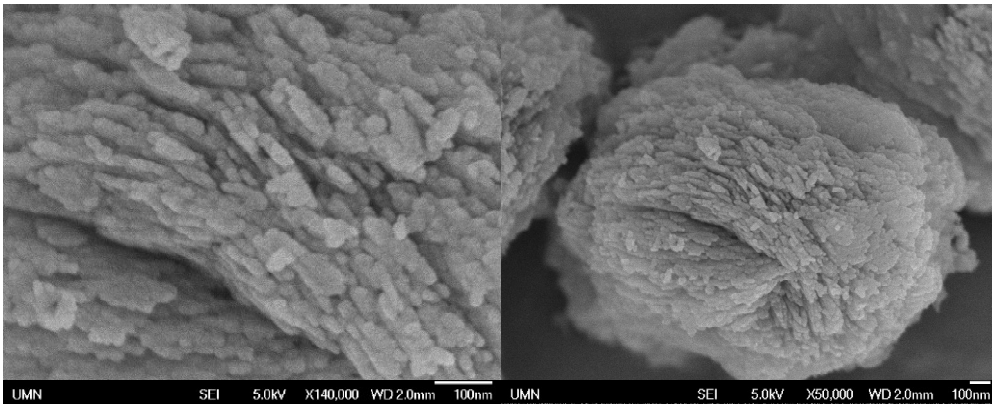


Figure 16: SEM Images of Silicalite-1 synthesized in 20 nm template

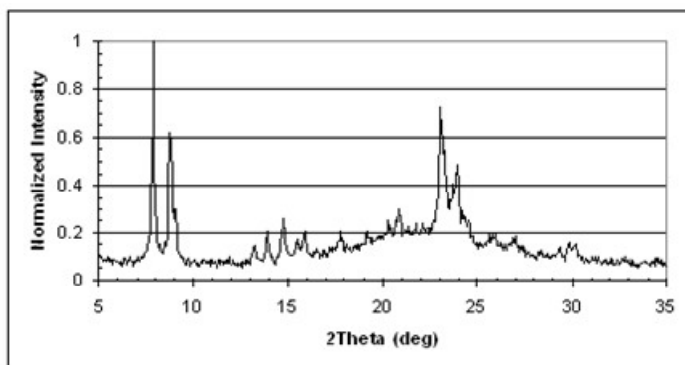


Figure 17: WAXD of silicalite-1 synthesized in 10 nm template

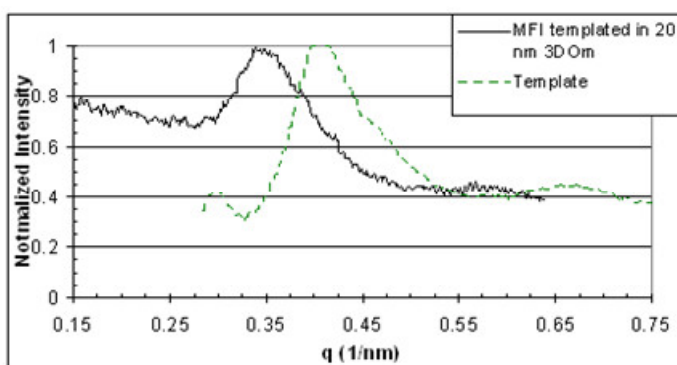


Figure 18: SAXD of templated silicalite-1 and template.

### 3.3 ZSM-5 by Inclusion of Aluminum Sources in SDA Solution

Aluminum can be introduced into the zeolite frame work to add catalytic activity to the synthesized material. Perhaps, the simplest method to introduce aluminum into the reaction mixture is to add an aluminum source to the SDA solution before introducing it into the template. Aluminum isopropoxide was chosen as the aluminum source because of its availability in the lab, ease of measurement and hydrolysis, and easily evaporated isopropanol byproduct.

A clear solution of 18 TPAOH/0.3 NaOH/390 H<sub>2</sub>O/1.25 Al<sup>+3</sup> can be generated after approximately an hour of mixing. This level of aluminum would result in a Si/Al ratio of

40, in solution. The problem comes upon the addition of ethanol to the growth solution. The solution displays only temporary stability once ethanol is added, becoming cloudy after ethanol addition, time for this effect is dependent on the amount of aluminum present. Dynamic light scattering can be utilized to show the formation of particles within solution, even though it still looks clear.

Alternative aluminum sources were investigated to determine if the formation of alumina particles in the SDA solution was related to aluminum isopropoxide. Alumina, aluminum triethoxide, aluminum flakes, aluminum tri-sec-butoxide, and aluminum sulfate hexahydrate all present a similar effect of forming alumina particles in solution when ethanol is added. This is a hindrance for incorporating aluminum within the zeolite framework grown within the carbon template. If alumina particles are stuck on the outside of the carbon template, too large to actually enter the pore system of the template, the aluminum cannot be incorporated in the framework.

### 3.4 ZSM-5 from Aluminum Isopropoxide

Early experiments by Dongxia Liu have shown the activity of ZSM-5 made from aluminum isopropoxide in the SDA solution had displayed lower activity than commercial zeolites in catalytic investigations. Further investigation suggests that samples did not incorporate all the aluminum introduced in the SDA solution. This problem potentially relates to the instability of alumina in solution when ethanol is added. In order to combat this problem, the ethanol was replaced with additional water. The purpose of the ethanol was to aid in introduction of the SDA solution into the carbon

template; however it had a detrimental effect when aluminum was included in the SDA solution.

In order to investigate whether the alumina particles present in the SDA solution caused by the addition of ethanol, was the hindrance to obtaining zeolites with a low silica to alumina ratio two samples were made using water as the secondary solvent. Following the mole ratio of 18 TPAOH:0.3 NaOH:50 SiO<sub>2</sub>:390 H<sub>2</sub>O:(1.25 Al<sup>+3</sup> (40), 2.5 Al<sup>+3</sup> (20)):180 H<sub>2</sub>O, where the second ratio of water is evaporated. TPAOH (40 wt%), 10 m NaOH, aluminum isopropoxide, and water were mixed in a conical tube to form the SDA solution. The SDA solution was then added volumetrically to dried carbon. The excess water was evaporated in the fume hood, water loss was followed by change in sample mass. After water evaporation, TEOS was added volumetrically to obtain the proper ratio. The vial was then placed in a Teflon liner with ~3 grams of water, and sealed in an autoclave. The sample aged for 3 hours. SAC was performed at 135 °C for 3 days. The sample was subsequently quenched in water.

Following SAC, the sample was washed with DI water on a filter pad (whatman 542). The structure directing agent was then decomposed by heating the sample to 550 °C for 8 hours under an inert atmosphere. This removes the structure directing agent but retains the carbon template. Following the decomposition of the structure directing agent, an ion exchange was performed to replace sodium with ammonium. Ammonium is the desired counter ion for the framework to form the hydrogen form of ZSM-5.

The sample then underwent four ion exchanges with ammonium nitrate, to exchange sodium for ammonium. The ion exchange was performed in a round bottom flask fitted

with a condenser with a 1 M solution of ammonium nitrate, heated to 80 °C for 4 hours. Following each ion exchange, the sample was washed with additional water. After completing the four ion exchanges, the template was removed. Template remove was performed by calcination in air at 500 °C with a slow ramp rate.

The samples were first characterized to ensure the crystallinity and morphology where as anticipated.

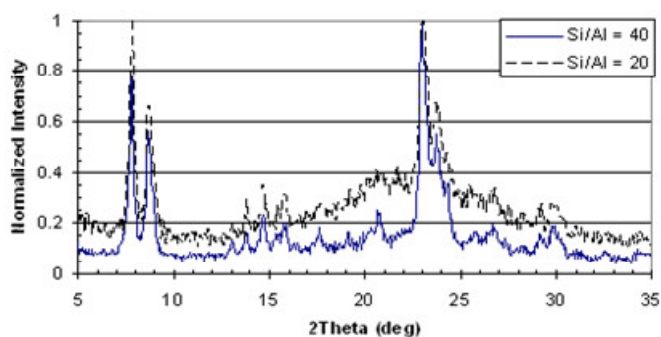


Figure 19: WAXD of Aluminum Containing MFI Samples

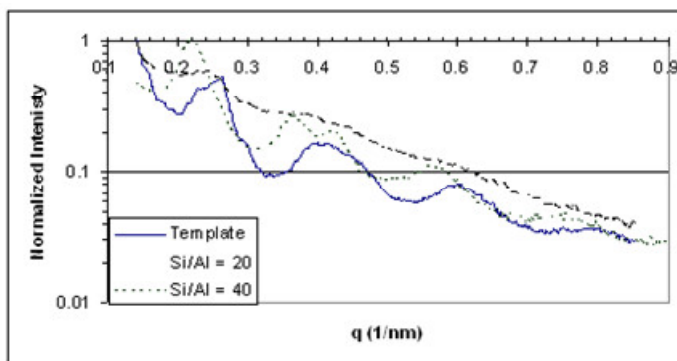


Figure 20: SAXD of Aluminum Containing MFI Samples

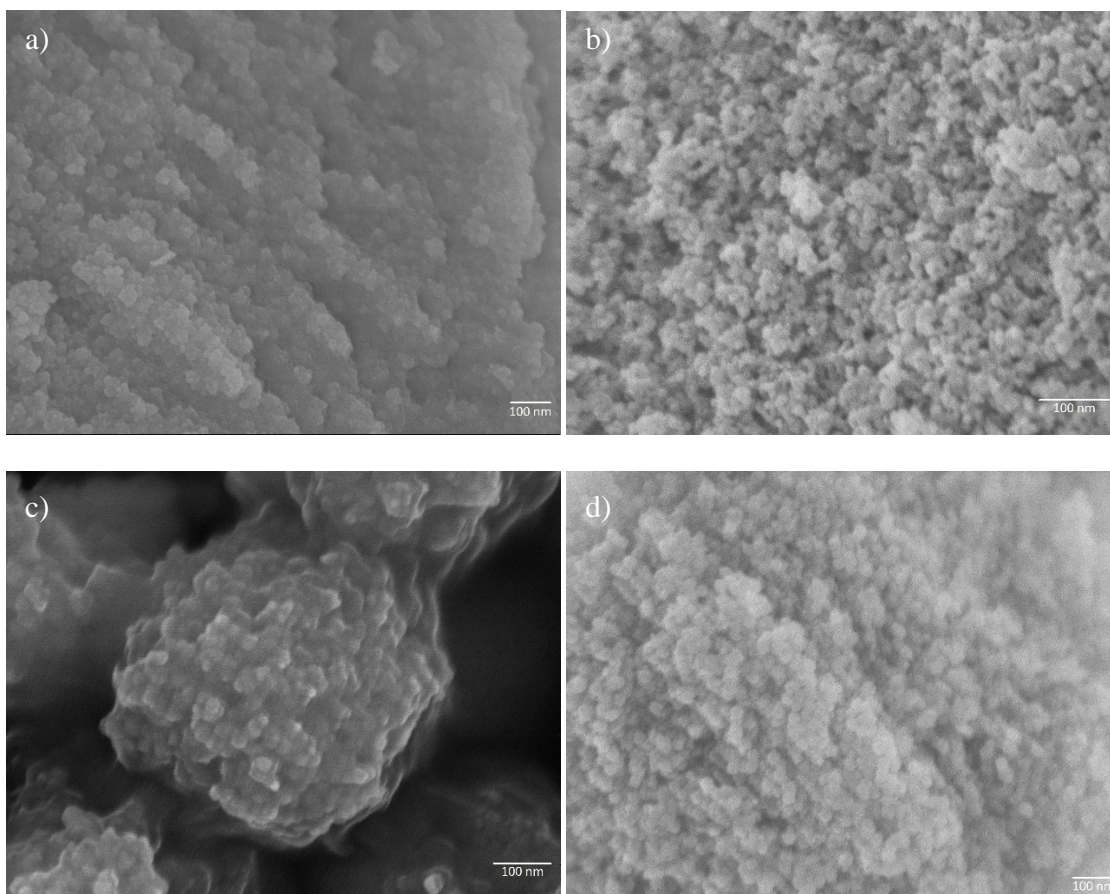


Figure 21: SEM Images a) and b) Si/Al = 20 and c) and d) Si/Al = 40

The characterization of the synthesized samples, reveals that the 3DOM-i Si/Al = 20 MFI sample displays lower crystallinity as well as poor colloidal crystal structure, when compared to the 3DOM-i Si/Al = 40 MFI sample. The relatively poor ordering of colloidal structure can be observed with SEM, which shows a poor stacking of spheres. The 3DOM-i Si/Al = 40 MFI sample has higher crystallinity as well as better colloidal structure, as indicated by the strong small angle diffraction peaks.

### 3.5 ZSM-5 Alternative Aluminum Sources

In order to prevent any difficulties from aluminum isopropoxide forming alumina particles in the SDA solution which hinders aluminum incorporation into the frame work within the template, an organic liquid form aluminum was chosen for investigation. Aluminum tri-sec-butoxide, is a viscous liquid aluminum precursor, which can be hydrolyzed to form aluminum within the template. Due to its high viscosity, aluminum tri-sec-butoxide needs to be diluted in solvent to accurately add to the carbon template. Aluminum tri-sec-butoxide can be dispersed in toluene and TEOS. Two samples were made, one using aluminum tri-sec-butoxide dispersed in toluene and the other dispersed in TEOS.

The aluminum tri-sec-butoxide dispersed in toluene sample, hereafter referred to as sample 1. Sample 1 was generated in 40 nm 3DOM carbon template. The carbon template was first impregnated with the mixture of toluene and aluminum tri-sec-butoxide. Time was given for the toluene to evaporate. The SDA solution was then volumetrically added to the template. Time was given to evaporate ethanol out of the template from the SDA solution. After removal of the ethanol, TEOS was added to the

sample. The sample was subsequently placed in a Teflon liner with approximately 3 g of water. The sample was aged for 3 hours, before being heated to 135 °C for 3 days.

The aluminum tri-sec-butoxide dispersed in TEOS sample, hereafter referred to as sample 2, and was also generated in 40 nm 3DOm carbon template. The carbon template was impregnated with SDA solution. The ethanol in the SDA solution was allowed to evaporate. Next TEOS mixed with aluminum tri-sec-butoxide in the desired ratio, was added volumetrically to the template. The sample was loaded into a Teflon liner with approximately 3 grams of water. The sample was aged for 3 hours before being heated to 180 °C for 1 day.

Following quenching, sample 1 and 2 were handled the sample as earlier MFI samples. After the subsequent ion exchange and calcination, each sample was characterized to look at morphology and crystallinity.

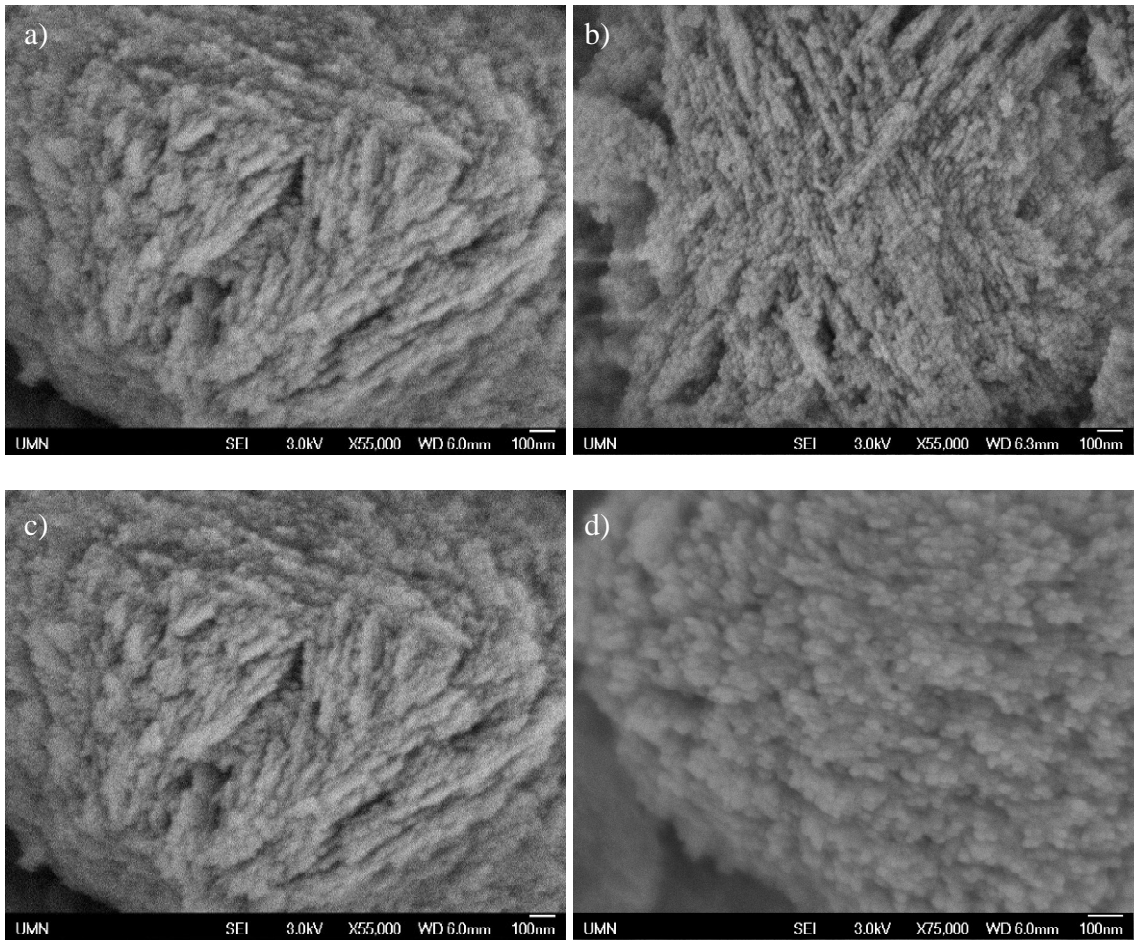


Figure 22: SEM images of sample 1 a) and b) and sample 2 c) and d)

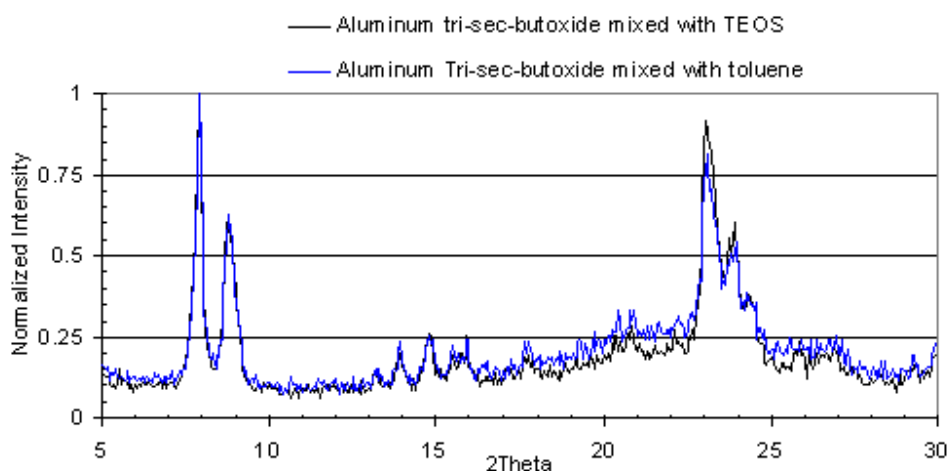


Figure 23: WAXD of Crystalline Samples

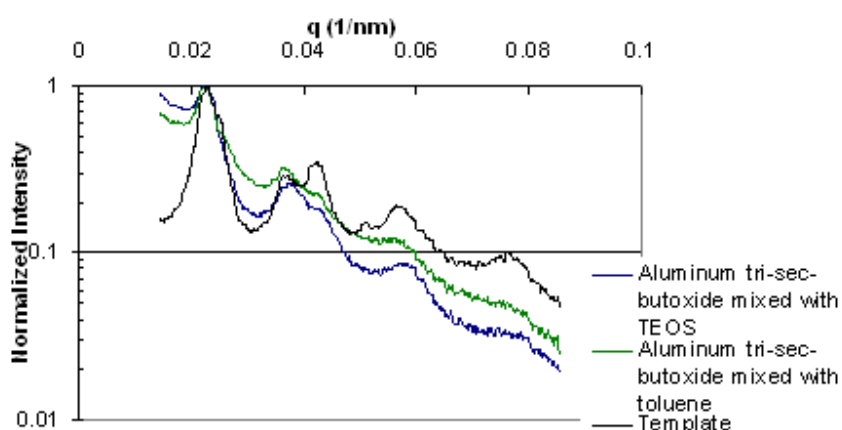


Figure 24: SAXD of Crystalline Samples

From this experiment, it can be shown that the MFI structure can be formed within the template when aluminum is incorporated into the template through this organic liquid aluminum source.

### 3.6 Importance of Water in Template for Silicalite-1 Synthesis

In order to get a better understanding of the importance of water on the crystallization behavior of silicalite-1 within the 3DOM template three samples were made to

investigate the importance of water. The first sample utilized the 3DOm template like previous sample, however the water was evaporated out of the template at 70 °C overnight. This sample was compared with control samples, where the growth materials were added to a vial without the presence of the carbon template. One of these samples was then dried to form a dry gel, while the other was not dried leaving all the water within the vial.

Each sample was made to the mole ratio of 18 TPAOH:0.3 NaOH:50 SiO<sub>2</sub>:390 H<sub>2</sub>O. The water could then be evaporated using an oven at 70 °C. The sample vials were placed in a Teflon liner with approximately 3 g of water, and sealed in an autoclave. The vials were heated to 135 °C for 3 days. After 3 days the autoclaves where taken out of the oven and rapidly quenched in water. Upon cooling the sample vials could be removed, and the sample extracted for calcination. The samples where calcined in air at 550 °C to remove the template and structure directing agent. The samples where then characterized with SEM and WAXD.

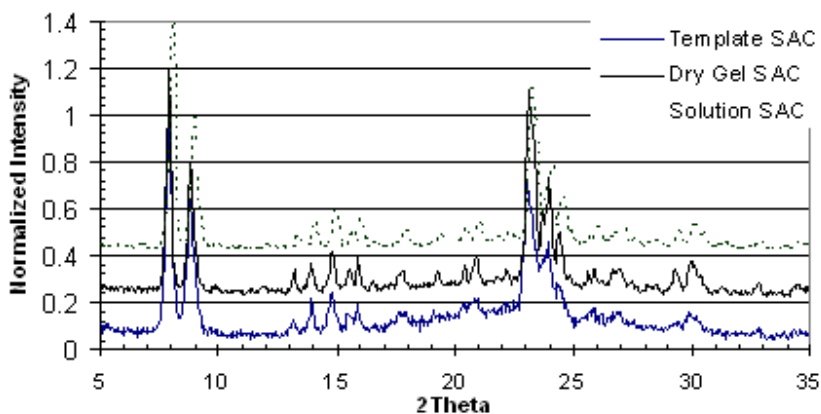


Figure 24: WAXD of Sample Series

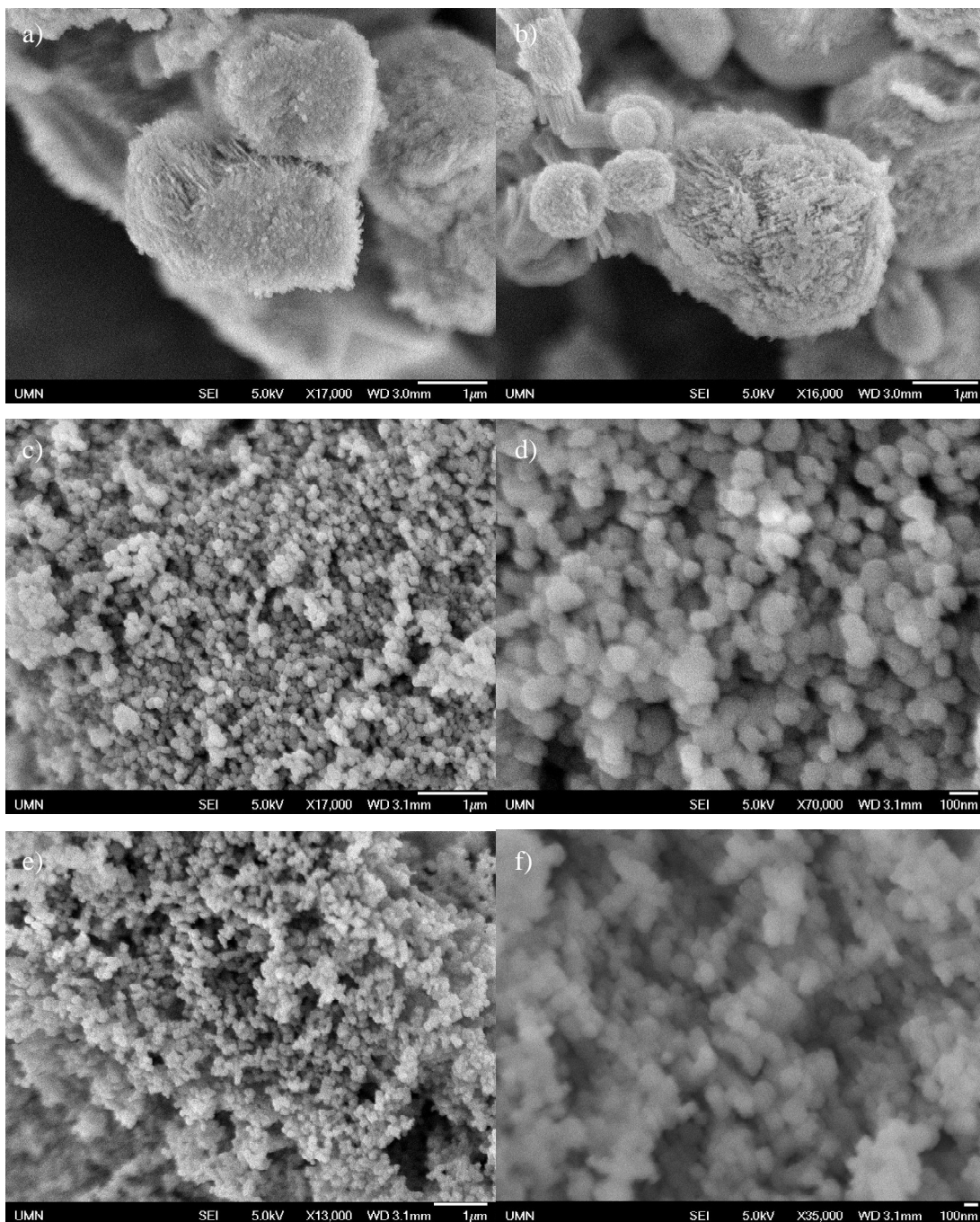


Figure 25: SEM of Particle Morphology: a) and b) 3DOm-i MFI from Dried Gel, c) and d) MFI from Dry Gel, and e) and f) MFI from Solution Under SAC

Based on the results from the WAXD it can be observed that each sample successfully produced the MFI crystalline phase. This is not very surprising since MFI is fairly easy to crystallize, but it does prove that water is not necessary for the SAC method utilized here to generate 3DOM-i.

The SEM proved more interesting data, while water is not needed to form the MFI crystalline phase within the template, it does have an important effect on its morphology and nucleation. While not very clear in the SEM images present, you need to consider the focal plain behind the 3DOM-i particle, there was a significant amount of large faceted crystals. This is different from all previous results presented showing the formation of 3DOM-i MFI. The water in the sample appears to aid in maintaining crystal growth within the template. It should be noted that this experiment was only performed once, and optimization may be able to help generate less exterior template growth.

The control samples also present interesting information about the sample. After seeing faceted crystals in the template sample, one would expect to also see faceted crystals in the control samples since there is no template to limit growth and force a 3DOM morphology. However, both control samples did not result in large faceted crystals, their particle morphology was spherical with a diameter of approximately 100 nm. This result displays that the carbon has a large effect on the nucleation and growth of zeolite particles. The larger particles, collection of 40 nm particles in the 3DOM structure, from the template sample are much larger than that produced when no template is present.

## Chapter 4

### Attempted synthesis of 3DOM-i Beta crystals

#### 4.1 BEA goal

The focus of my research has been to synthesize zeolite Beta within the 3DOM template. The structure of Beta makes it highly desirable for catalytic applications in industrial scale reactions. This interest in potential catalytic applications has driven research into methodologies of synthesizing crystals with varying sizes and degrees of dispersion.

Zeolite beta is known as a disordered structure composed of two polymorphs termed polymorph A and B. Beta is often characterized as having stacking faults between successive planes. ABCABC... sequences are often interrupted by sequences of ABAB..., BCBC..., or CACA...<sup>22</sup>. The layer units of the Beta structure undergo a lateral shift of  $\pm 1/3a$  or  $\pm 1/3b$ , the lateral repeat distance.<sup>20</sup> The probability of a stacking fault in the ABC sequence is approximately 0.3 to 0.45<sup>22</sup>.

Polymorph A is tetragonal symmetric with  $a = 1.249$  nm and  $c = 2.644$  nm, where the cages are arranged in a helical fashion around a 4 fold screw axis that can be either right or left handed<sup>22</sup>. This symmetry allows polymorph A to exist as an enantiomeric pair. Polymorph A has an ABAB stacking arrangement. The two enantiomeric sequences follow RRRR... sequence for  $4_1$  or LLLL... sequence for  $4_3$  related to the screw axis.<sup>21</sup>

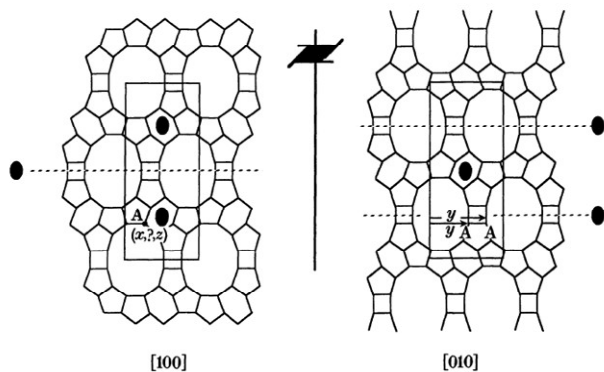


Figure 26: Beta Polymorph A symmetry elements<sup>19</sup>

Polymorph B has monoclinic symmetry where  $a = 1.764$  nm,  $b = 1.781$  nm,  $c = 1.44$  nm, and  $\beta = 114.5^\circ$ , and alternates in handedness resulting in an achiral structure<sup>22</sup>. The stacking of Polymorph B follows ABCABC... Due to the glide operation between stacks, the sequence alternates handedness RLRLRL..., resulting in an achiral structure<sup>22</sup>.

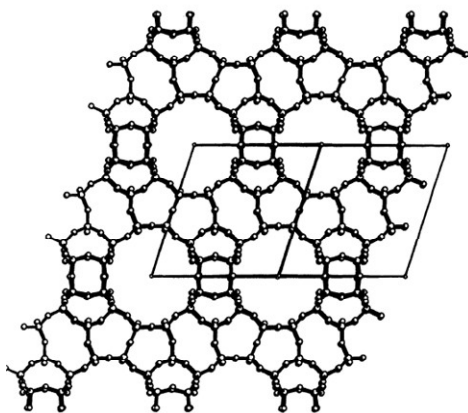


Figure 27: Beta Polymorph B viewed along  $[110]$ <sup>22</sup>

The Beta structure contains two 12 member rings. One ring is  $6.6$  by  $6.7$  Å along the  $\langle 100 \rangle$  plane. The second ring is smaller at  $5.6$  by  $5.6$  Å along the  $[001]$  direction<sup>23</sup>. The large pore diameter of zeolite Beta makes it of interest for catalysis. A material

synthesized of pure Polymorph A has potential for chiral catalysis due to the chiral nature of its pore<sup>22</sup>.

Due to the disordered nature of the Beta Structure, x-ray diffraction patterns are composed of both broad and sharp peaks. The relative amounts of each polymorph influence the observed pattern, as shown in the figure 17.

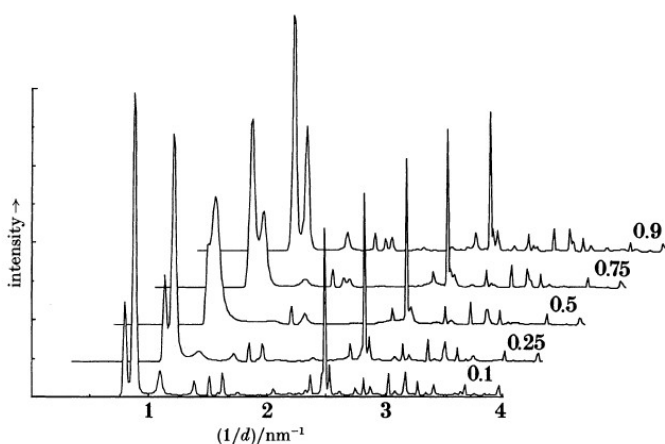


Figure 28: Computed x-ray diffraction patterns for Beta with different amount of Polymorph A and B, where 0.9 is mostly Polymorph B<sup>22</sup>

#### 4.2 SAC from aluminum isopropoxide SDA solution

Initial attempts at synthesizing Beta within the 3DOM template have relied upon using aluminum isopropoxide mixed with the structure directing agent. This combination of aluminum source and structure directing agent would be diluted prior to impregnation into the carbon template. The BEA recipe utilized called for a mole ratio of starting material of: 1.6 Al<sub>2</sub>O<sub>3</sub>:15.7 TEA<sub>2</sub>O: 2.3 Na<sub>2</sub>O: 50 SiO<sub>2</sub>: 510 H<sub>2</sub>O to be introduced into the template. This recipe was based off of the work of Schmidt who claimed to demonstrate BEA crystallization under steam assisted growth.<sup>24</sup> Initial focus was on the utilization of ethanol as the secondary solvent to facilitate the impregnation of the carbon

with this aqueous mixture. Using ethanol as a secondary solvent, a solution of alumina, tetrethylammonium hydroxide, sodium hydroxide, water, and ethanol were added to the carbon template. The ethanol was then evaporated off from the template in a fume hood. TEOS was then added to the template as the silica source. The impregnated template was then place in a Teflon liner containing approximately 3 grams of water, which would act to form a saturated steam environment upon heating, and sealed in a stainless steel autoclave. The sample was allowed to age for 3 hours before being heated to 140 °C for 6 days. The autoclave was subsequently quenched in water to cool. The sample could then be removed and calcined to remove carbon at 550 °C in air for analysis.

This recipe was attempted several times, however there was never any crystallization of an ordered material, BEA or otherwise. The samples were characterized by WAXD to determine crystallinity and SEM to investigate the morphology of the product. WAXD only showed a large amorphous peak. SEM could be used to confirm the formation of small particles; however they had no ordering to them matching the 3DOm structure.

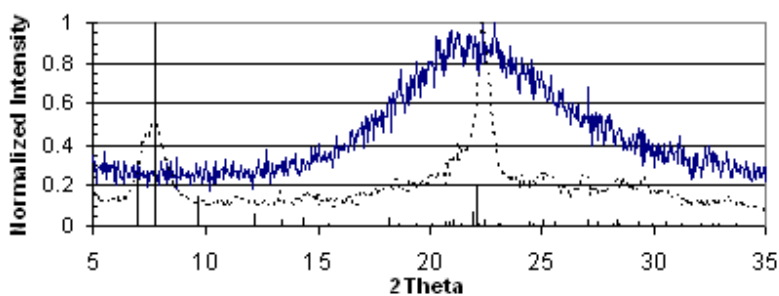


Figure 29: Representative experimental result with commercial sample and model diffraction lines

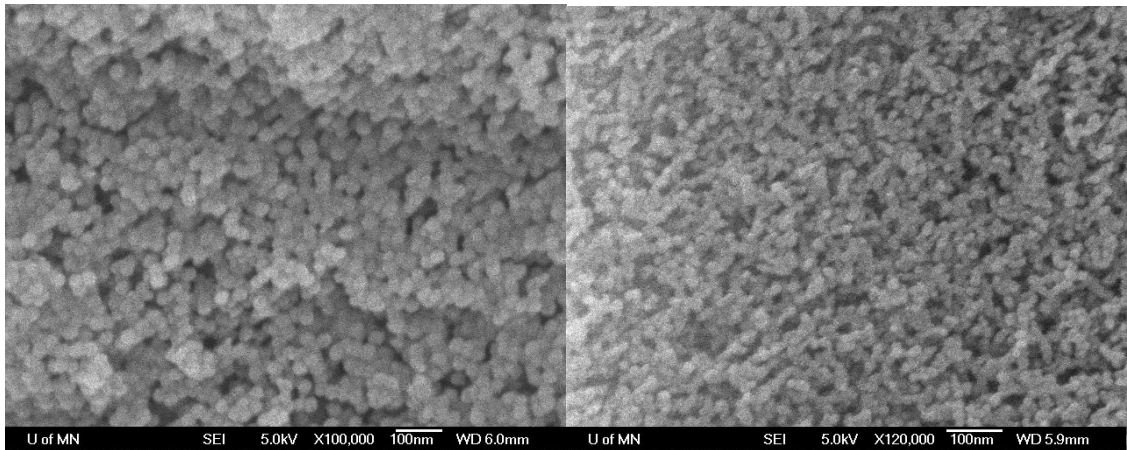


Figure 30: SEM of representative sample result

From the WAXD scan, it is clear there is no crystalline BEA phase present in the sample. The only peak arises from amorphous silica present after calcining the sample. SEM shows a lot of small particles, approximately the size of the template, which suggests the silica and alumina are able to enter in the template. The lack of 3D structure suggests that during hydrothermal heating, the alumina and silica simply precipitate where they are and don't form a growing crystal.

After several failures at synthesizing 3D*Om*-i BEA in this manor, the ethanol was removed from the synthesis solution and replaced with additional water to act as the secondary solvent. This experiment, like the pervious one, did not result in crystallization of a zeolite phase. SEM used shows a similar formation of small particles.

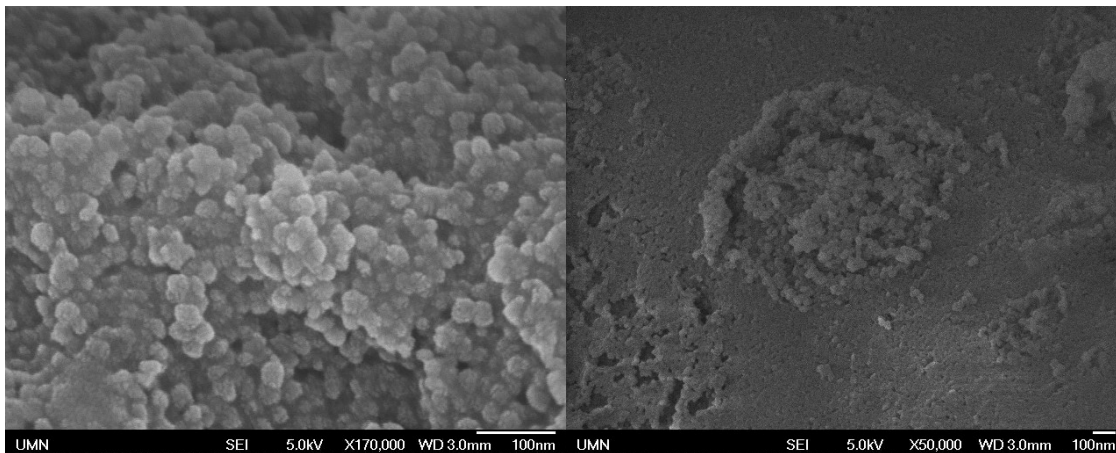


Figure 31: SEM images from attempted synthesis of 3D Om-i BEA using water as secondary solvent

#### 4.3 Dry gel SAC

An alternative method to generate zeolite Beta is to utilize a dry gel recipe. This method relies on forming a dry gel within the template structure, that can be turned into zeolite upon application of steam assisted crystallization. The idea is very similar to previous attempts, except that the water used to generate the gel will be evaporated before undergoing SAC.

A recipe previously published for dry gel synthesis of zeolite Beta was modified for use within the carbon template. Based off of the work by Sakthivel<sup>25</sup>, a synthesis gel was generated from tetraethylammonium hydroxide, alumina, silica, and sodium. The mole ratio of components in final mixture were calculated to be 1 SiO<sub>2</sub>:0.37 TEAOH:0.072 NaOH:0.0192 Al<sub>2</sub>O<sub>3</sub>:17 H<sub>2</sub>O. Upon mixing the reagents, the sample was heated to 70 °C to evaporate water, producing a dry powder.

After drying the gel was placed in a glass vial, to isolate it from the water utilized to generate the saturated steam environment. The vial was placed in a Teflon liner with

approximately 3 grams of water. The liner was sealed in a stainless steel autoclave, for high temperature treatment. The autoclave was placed in the oven at 175 °C for 1 day. After 1 day, the autoclave is rapidly quenched in water. The vial can then be removed from the liner, and the sample calcined for analysis.

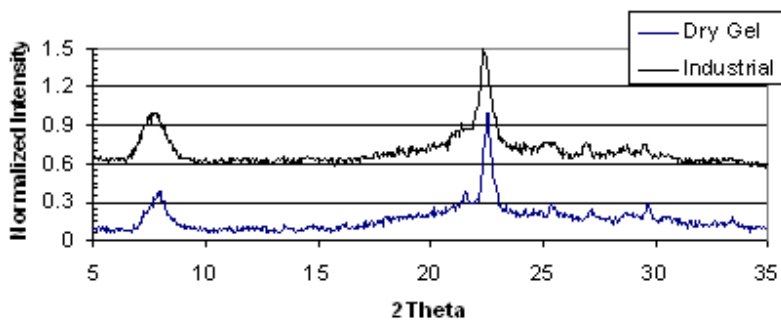


Figure 32: WAXD of Industrial Sourced BEA and Experimental Dry Gel Sample

Based off of the WAXD this method can be used successfully to generate zeolite Beta from the dry gel. The next step involves transitioning this dry gel methodology to include the use of a carbon template in the synthesis.

#### 4.4 Templated dry gel attempts

In order to synthesize zeolite BEA within the 3DOM template from this dry gel recipe some modifications needed to be made. The SDA solution needs to be diluted with ethanol to facilitate the incorporation of the SDA within the carbon. The aluminum source utilized was changed from aluminum isopropoxide to aluminum tri-sec-butoxide. Aluminum tri-sec-butoxide is a viscous liquid, unlike aluminum isopropoxide which is a solid. Due to the viscosity of aluminum tri-sec-butoxide it needed to be mixed with toluene or TEOS to form a mixture with a viscosity that lends its self to volumetric measurements.

Samples were generated by first drying the 3DOm carbon overnight. The carbon was then massed into a vial which could be inserted into the Teflon liner. If the aluminum tri-sec-butoxide was mixed with toluene, it would be added first followed by the SDA ethanol solution. When aluminum tri-sec-butoxide was mixed with TEOS, it is added at the end with the TEOS. The next addition is the SDA ethanol solution. The sample is then placed in the hood to evaporate the ethanol. The ethanol evaporation can be monitored by observing the change in mass of the vial and sample. After the ethanol is evaporated, the TEOS can be added to the sample.

Following the addition of the reaction materials, the sample was covered with parafilm and allowed to sit for 4 hours to allow mixing within the template. The sample was then warmed to 70 °C overnight to remove any water and ethanol that may be present. The vial can then be placed in a Teflon liner with approximately 3 grams of water. The liner is then sealed in a stainless steel autoclave and heated to 175 °C for 1 day.

Following this general method, several attempts were made to synthesize BEA within the 3DOm template. Unfortunately, all the experimental samples did not show any crystallinity. Oddly enough, in some cases the control samples did not generate any zeolite BEA even though the exact same process was followed batch to batch. Below are the results from one series of experiments that exemplify the results obtained in many experiments.

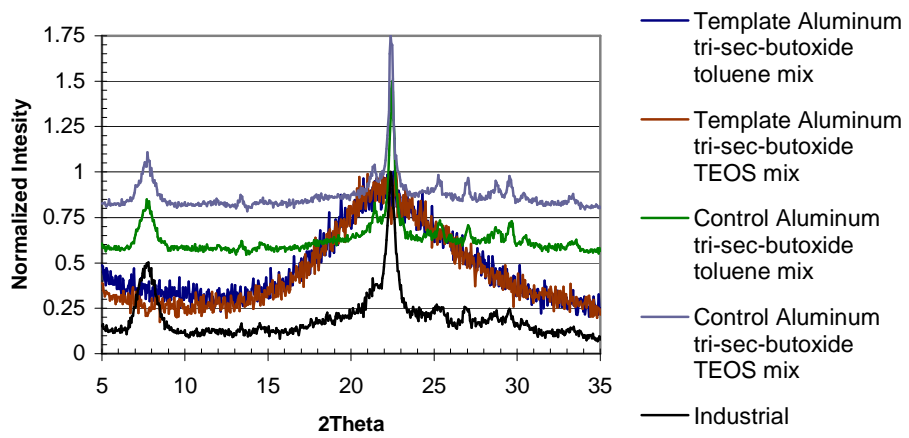


Figure 33: WAXD of 3DOm BEA sample series

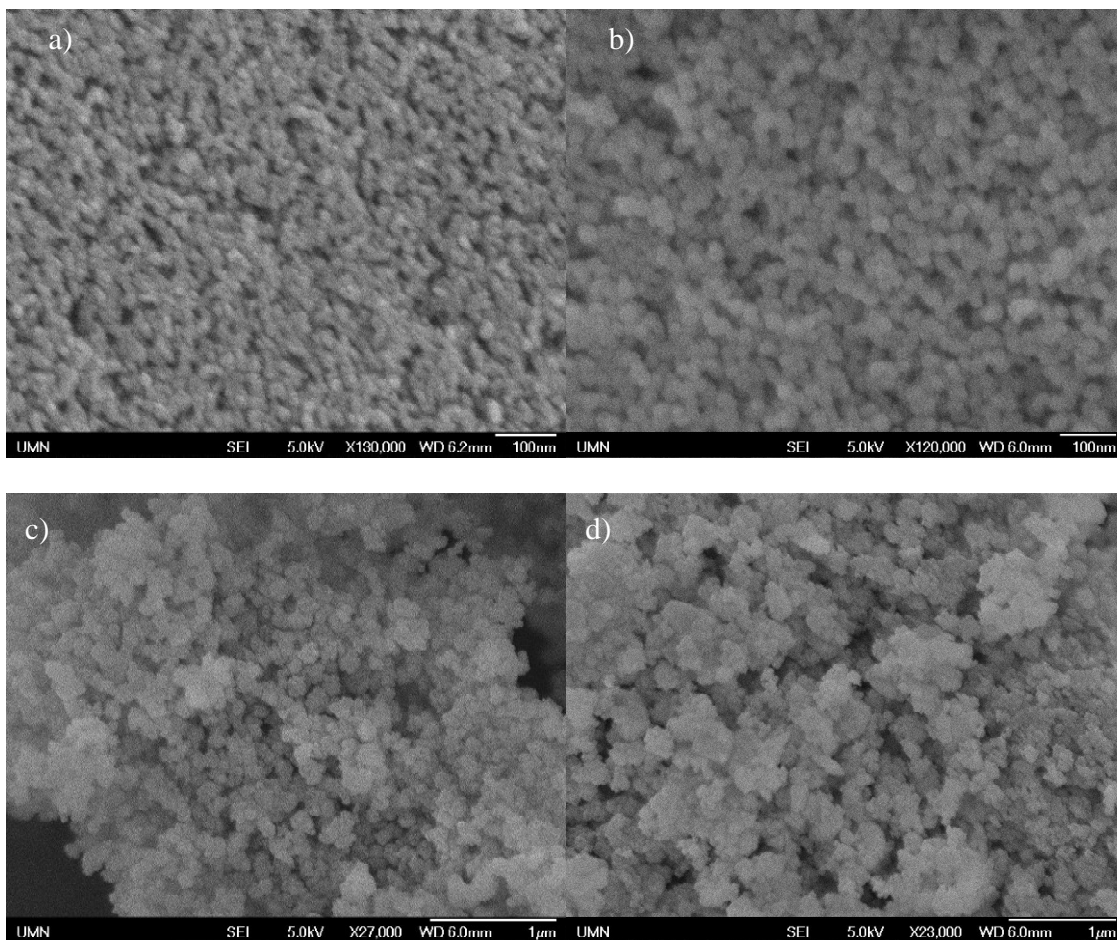


Figure 34: SEM Images from Series Samples: a) Aluminum tri-sec-butoxide with toluene mix, b) aluminum tri-sec-butoxide with TEOS mix, c) control aluminum tri-sec-butoxide with toluene mix, d) control aluminum tri-sec-butoxide with TEOS mix

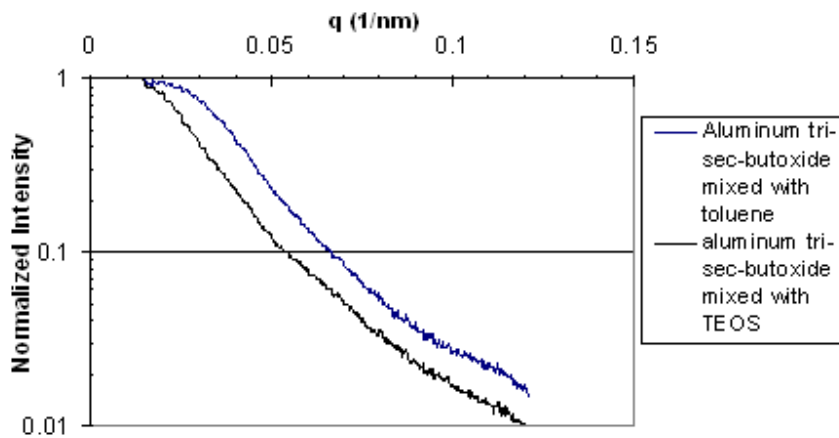


Figure 35: SAXD Pattern for Template Samples

From the results it can be seen that the carbon impacts the size of the particles form, which is part of the desired effect. The particles however do not take on the 3DOm structure that is desired.

#### 4.5 Large carbon synthesis

In order to investigate whether the template pore size is the cause of the lack of crystallization, large pore carbon template was generated. The large pores of this template, approximately 300 nm, should be large enough to allow crystal formation. The same recipe from the previous series of experiments was utilized, only changing the size of the pore size of the carbon template.

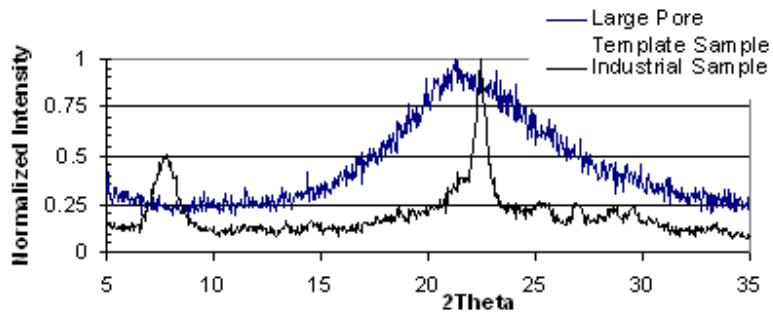


Figure 36: WAXD of Large Pore Template Sample with Industrial Sourced Material

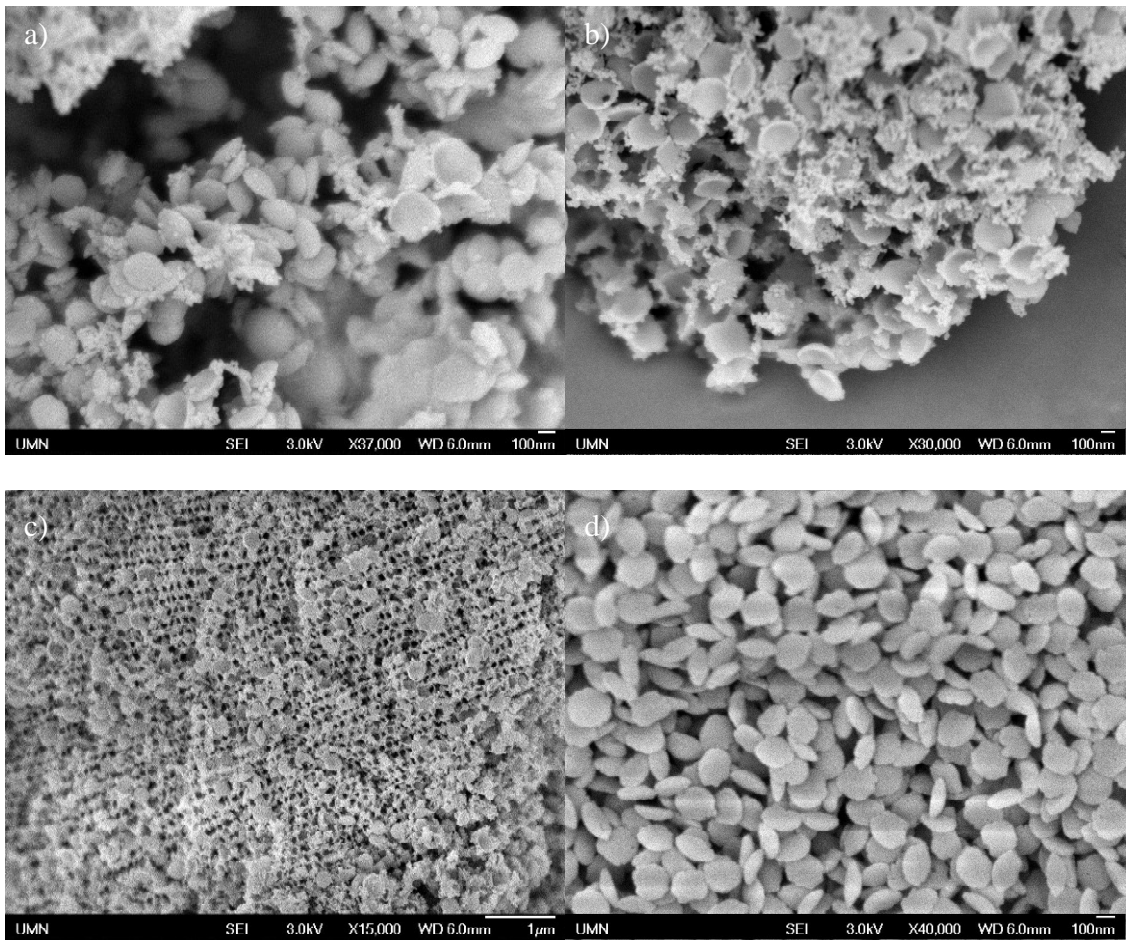


Figure 37: SEM Images of Calcined Sample from Large Pore Carbon

While the WAXD determined that there was no crystalline phase present, the SEM revealed a variety of particle morphology based on how the silica and alumina source hydrolyzed and then were affected by the steam assisted growth phase. The particle morphology can be oval disc-like particles approximately 200 nm in diameter or smaller more spherical particles that can coalesce together along the walls of the 3DOM template.

## Chapter 5

### Synthesis of 3DOm-i LTA zeolite

#### 5.1 LTA structure

The Linde Type A (LTA) structure, commonly referred to as Zeolite A, is an aluminosilicate zeolite composed of sodalite cages connected by double four rings. The connected sodalite cages generate a cubic structure, which contains an 8 member ring that forms a pore with a diameter of 4.1 Å.<sup>20</sup> These pores generate channels that run through the structure in 3 directions.

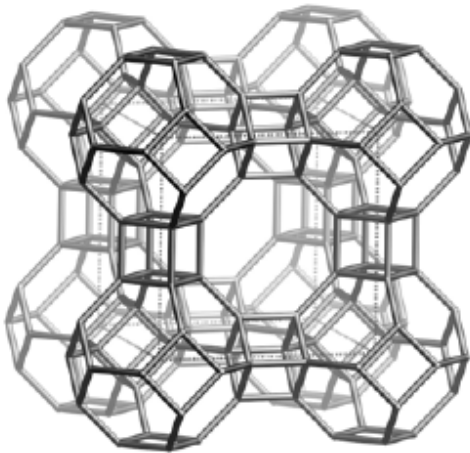


Figure 38: LTA structure, drawn along the [100]<sup>20</sup>

The chemical composition of the LTA aluminosilicate  $\text{Na}_x(\text{H}_2\text{O})_{216}\text{Al}_x\text{Si}_{192-x}\text{O}_{384}$  where  $x$  is the amount of alumina incorporated into the framework.

#### 5.2 Solution synthesis of 3DOm-i LTA

3DOm-i LTA is formed using a solution method of multiple infiltration and growth cycles to develop the zeolite crystal within the carbon template. The growth solution utilized for the reaction is a clear solution consisting of precursor materials. Silicic acid

is utilized as the silica source. Aluminum isopropoxide is used as the alumina source in the synthesis. Tetramethylammonium hydroxide is used as the structure directing agent. To generate the growth solution, tetramethylammonium hydroxide (25 wt% solution in water), 10 m NaOH, water, and silicic acid are added to a small bottle. The bottle is heated to 70 °C while mixing to aid in the dissolution of silicic acid. After the solution becomes clear, approximately 1 hour at 70 °C, the reaction mixture is cooled to room temperature. Aluminum isopropoxide is added to the solution in two separate additions of equal mass, giving time to mix to dissolve the solid between additions. After the aluminum isopropoxide is dissolved, the solution is aged while mixing for 1 hour. During aging the solution becomes cloudy, in order to remove the precipitated material formed during aging, the solution is filtered. The solution is vacuum filtered over a 542 Whatman filter pad, to form a clear solution. This clear solution can be stored for up to 48 hours without zeolite formation at room temperature. The solution may precipitate out a clear hydrated crystal over time, but this can readily be returned back into solution by mixing and slightly warming the solution. The materials are mixed to obtain a final ratio of 0.3187 Al<sup>+3</sup>:1 Si<sup>+4</sup>:0.0758 NaOH: 2.37 TMAOH:61.373 H<sub>2</sub>O before filtration.

3DOm carbon was placed into a Teflon liner or a conical tube with Teflon tape to aid in sealing the vessel, a conical tube can be utilized for this synthesis because growth occurs at 70 °C which is below the melting point for the plastic and does not generate a very high pressure. The growth solution is then added on top of the carbon. The system is aged for 1 hour at room temperature before heating to 70 °C in an oven. After 12 hours, the vessel is removed from the oven and cooled to room temperature. The carbon

is collected from the growth solution by filtering on a 542 Whatman filter pad. Water is used to wash the carbon to remove any external zeolite particles. This growth recipe results in small particles that can pass through the filter pad. The washed carbon is then placed in a cleaned liner or tube. Fresh growth solution is then poured on top of the carbon, and again aged for 1 hour before 12 hours of growth at 70 °C. The cycle of growth and washing is repeated 5 times to generate zeolite within the template.

Following the 5<sup>th</sup> growth cycle, the 3DOm carbon with zeolite is extensively washed to remove any exterior zeolite. The carbon is placed into a plastic bottle then immersed in DI water. The bottle is heated to 70 °C for 3 hours. The carbon is then isolated through vacuum filtration. This wash cycle is repeated 5 times to remove any exterior zeolite. Following the washing, the carbon is calcined to leave only the zeolite product. The zeolite can be characterized to ensure the reaction was successful.

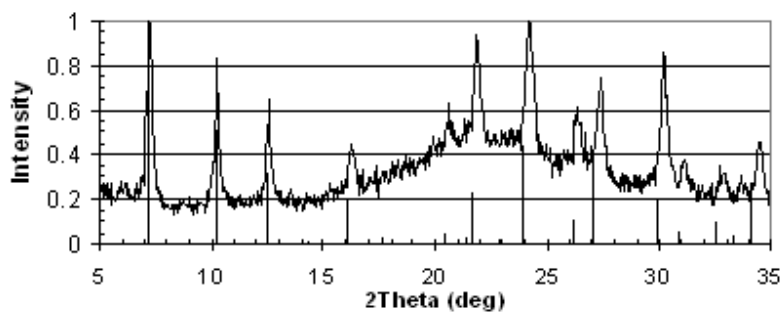


Figure 39: WAXD of produced zeolite along with predicted diffraction line positions

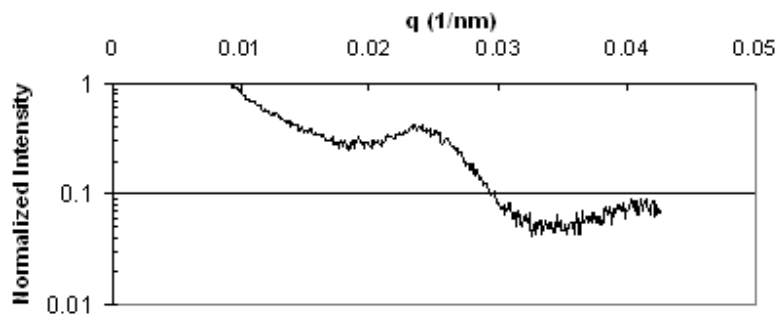


Figure 40: SAXD of produced material

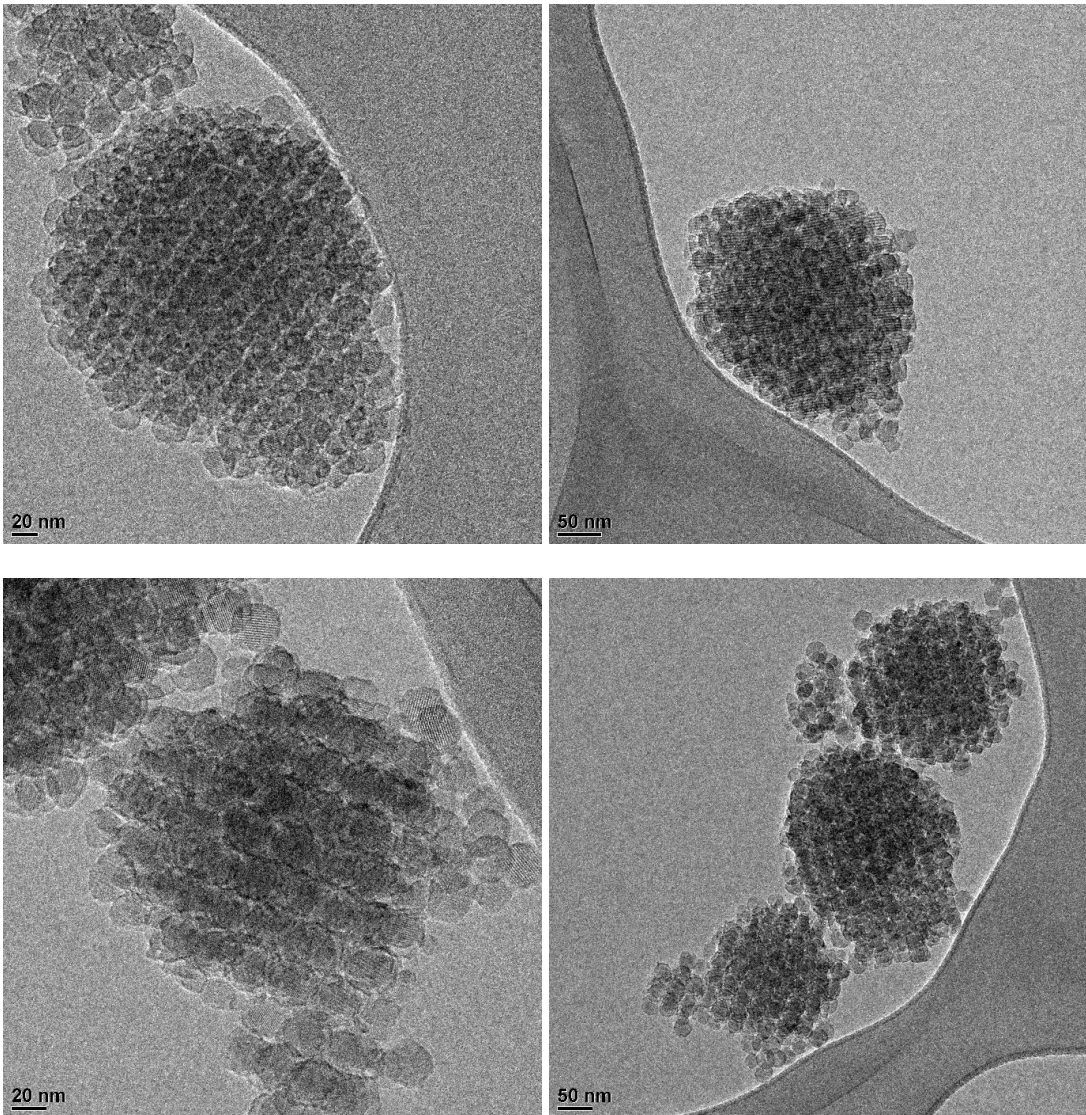


Figure 41: TEM Image of 3DOM-i LTA (image by Xueyi)

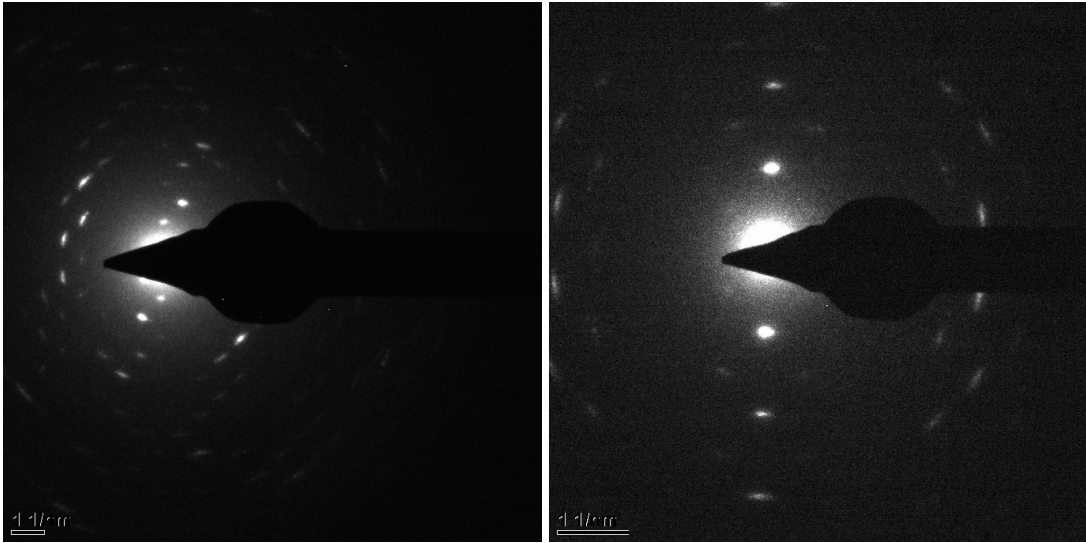


Figure 42: Electron diffraction taken from the 3D0m-i LTA sample (Courtesy of Xueyi)

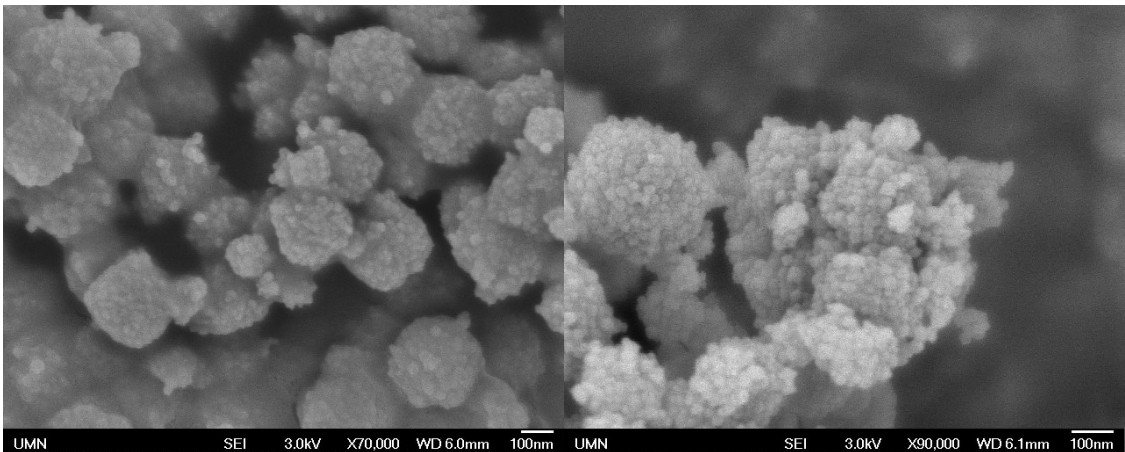


Figure 43: SEM images of 3D0m-i LTA

WAXD shows the anticipated peaks for the LTA structure, shown with model lines. Electron diffraction was also performed to confirm the LTA structure, not show. SAXD, SEM, and TEM are utilized to confirm the mesoporous structure of the zeolite crystal.

After the successful formation of 3D0m imprinted LTA particles, it was considered what makes this solution recipe capable of forming these particles. The recipe needs to form LTA particles that are small enough to be easily washed away from the outside of

the carbon, so a colloidal recipe seems appropriate for this restriction which this recipe forms. The particles also need to be LTA, which is clear from WAXD. In order to investigate the size of the crystals in solution, the wash liquid with dispersed particles was collected. The colloidal particles were collected through centrifugation of the wash liquid. The clear liquor was then decanted off the particles. The particles were subsequently dispersed in water to wash the particles and then collected again through centrifugation. After washing the particles until the wash water was a pH of approximately 7, the particles could be analyzed.

The particle size was measured by DLS while dispersed in water. The DLS result indicates a size of 127 nm based on Brookhaven's software. The software also determines a polydispersity of 0.028.

The results from the DLS measurements are confirmed by analyzing the sample also with SEM. After drying the particles, the particles could be analyzed as a powder with SEM. The particles found by SEM have a size of approximately 130 nm, and generally look monodisperse.

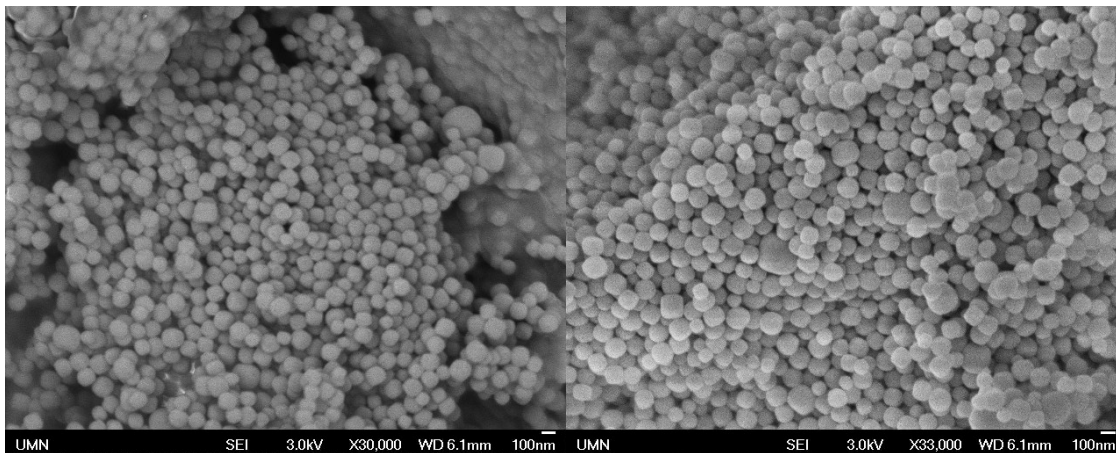


Figure 44: SEM of LTA particles from solution

### 5.3 MFI Growth on 3DOm-i LTA

After the synthesis of 3DOm-i LTA, it was considered whether it is possible to synthesize MFI crystals within the mesopores of 3DOm-i LTA. In order to investigate this possibility 3DOm-i LTA was used as the template for steam assisted crystallization process as well as mixed with an MFI growth solution.

In order to use a steam assisted crystallization process to grow MFI within the 3DOm-i LTA, the same reaction mixture used for synthesis of 3DOm-i Silicalite-1 was modified to utilize additional ethanol to facilitate the transfer of growth material into the mesopores. This idea was attempted two times, once generating 3 mg of Silicalite-1 in 100 mg of 3DOm-i LTA and the other generating 10 mg of Silicalite-1 in 100 mg of 3DOm-i LTA. The recipe was modified by altering the concentration of SDA and TEOS within the diluent ethanol.

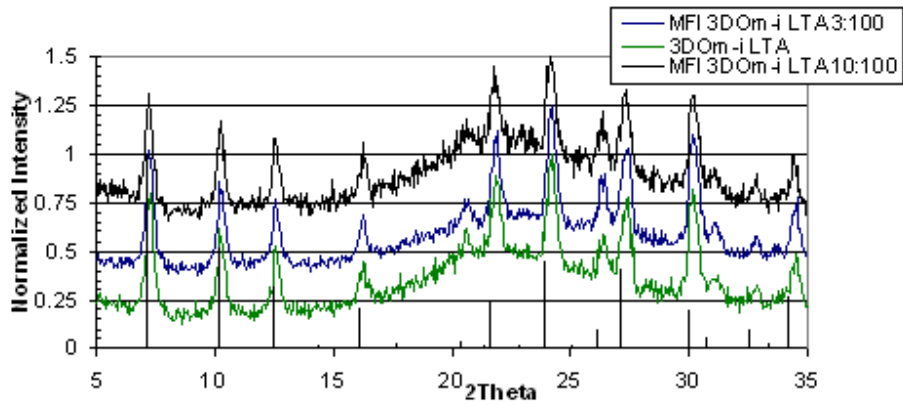


Figure 45: WAXD of synthesized samples

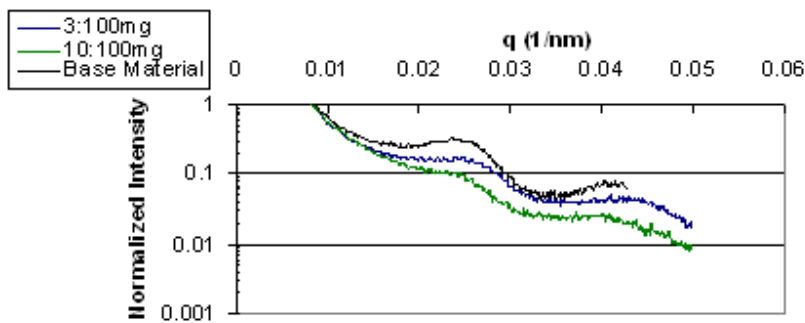


Figure 46: SAXD of synthesized samples

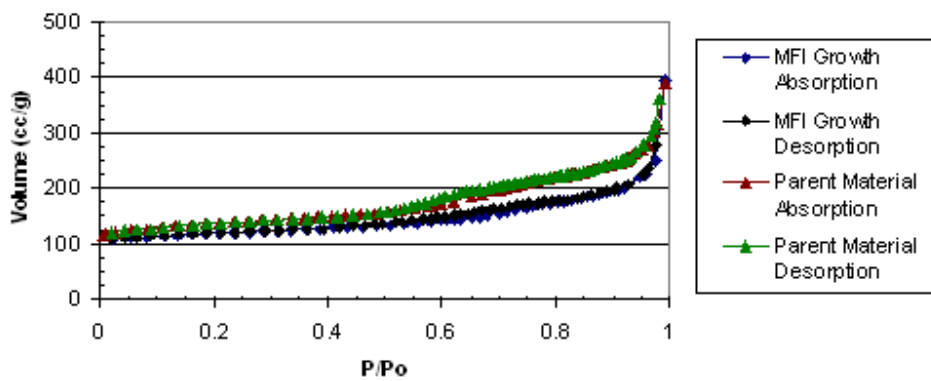


Figure 47: BET isotherms before and after SAC growth of 3:100 material

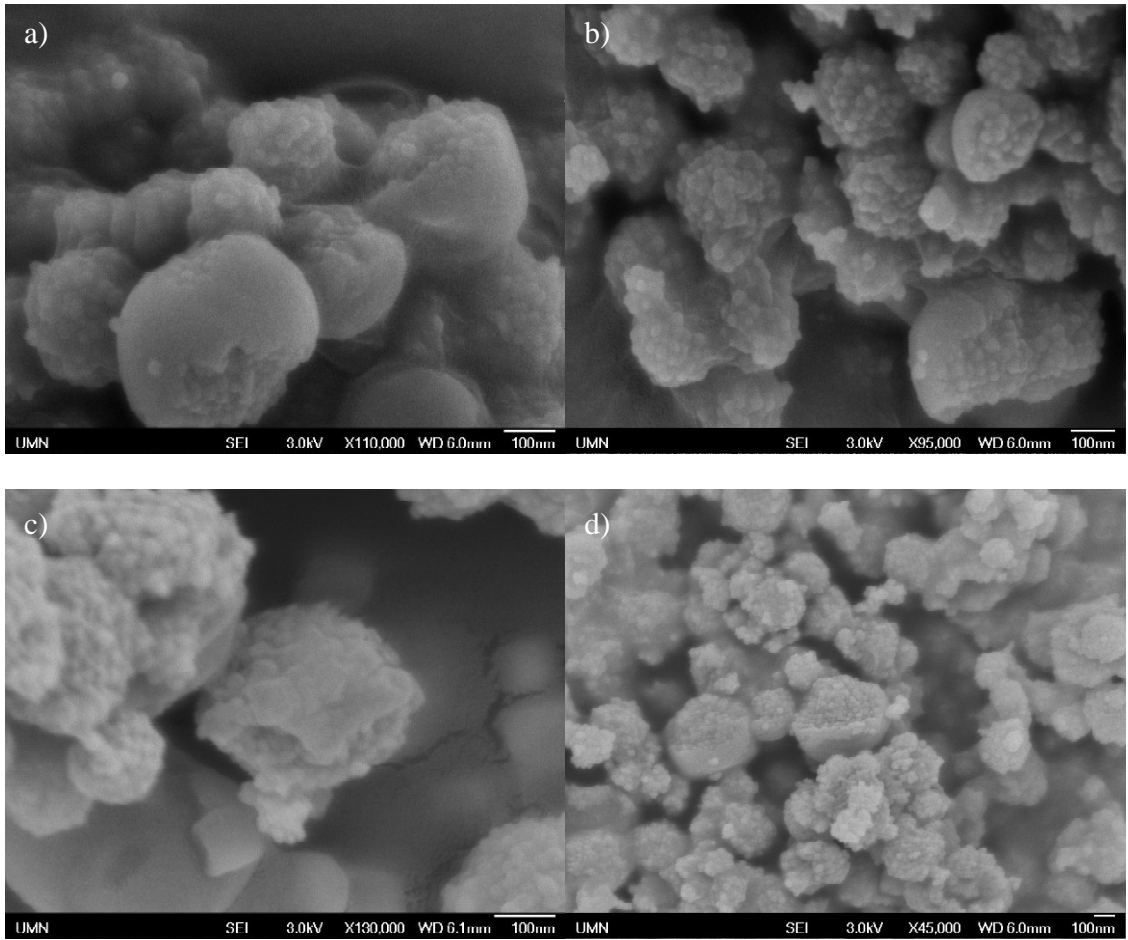


Figure 48: a and b 3:100 with c and d 10:100

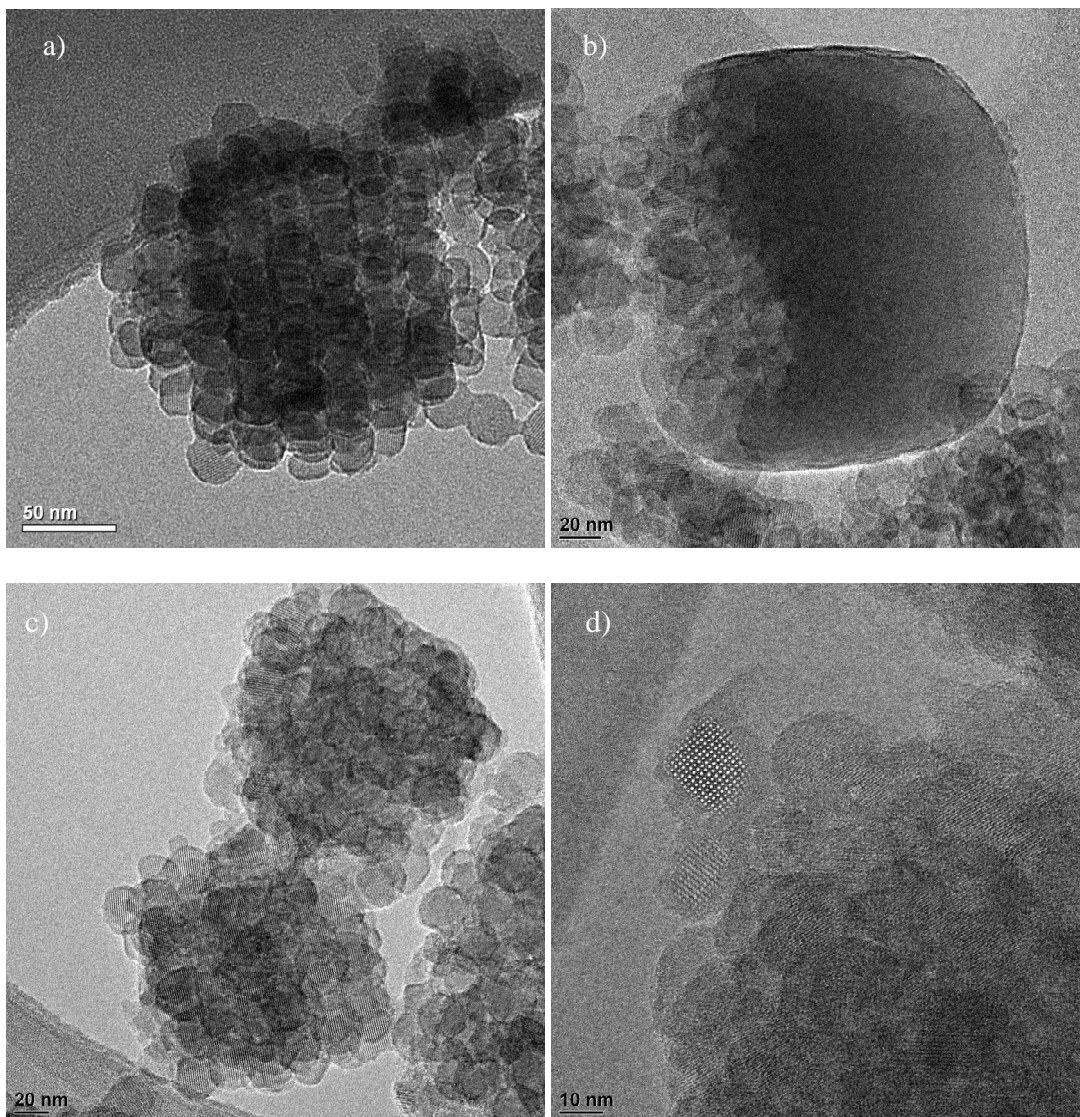


Figure 49: a) and b) 3DOM-i LTA with 3:100 mg ratio, c) and d) 3DOM-i LTA with 10:100 mg ratio (Courtesy of Xueyi)

The WAXD does not show any significant peak changes from the original 3DOM-i LTA structure, which indicates that the structure remains intact. The lack of any real MFI peaks in the 10 mg Silicalite-1 to 100 mg 3DOM-i LTA, is not a good indication of substantial formation of the MFI structure within the mesopores of the 3DOM-i LTA.

The SEM is rather interesting. While most of the sample retains the expected 3DOM imprinted morphology, there are sections where the 3DOM-i LTA seems to be covered with a smooth material. This smooth material introduced during the addition of MFI reactants is more prevalent in the higher MFI:LTA sample.

Additionally it was attempted to grow Silicalite-1 crystals within the mesopores of 3DOM-i LTA using a solution method. Using the C3 solution, published by Davis<sup>26</sup>, 10 mg of 3DOM-i LTA were added to approximately 5 mL of growth solution. The solution consisted of 20 SiO<sub>2</sub>:9 TPAOH:8100 H<sub>2</sub>O:480 EtOH, where the ethanol is derived from the silica source, tetraethyl orthosilicate, upon hydrolysis. Two samples were made at different temperatures: one sample at 70 °C for 2 days and the other at 135 °C for 1 day. During the reaction the samples were shaken by hand to ensure the 3DOM-i LTA particles were adequately dispersed in the solution. Following the reaction, the 3DOM-i LTA was isolated by centrifugation. The 3DOM-i LTA was then washed with water until the pH of the wash water remained approximately neutral. The samples were then characterized by WAXD and SEM.

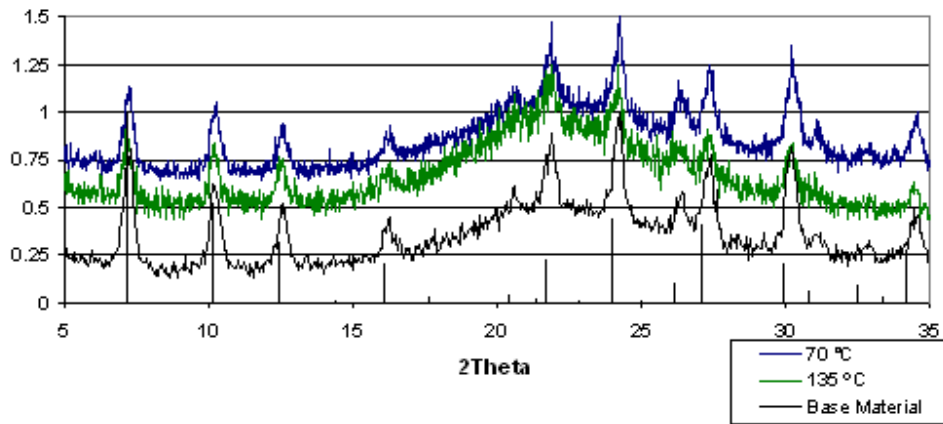


Figure 50: WAXD for samples and base material

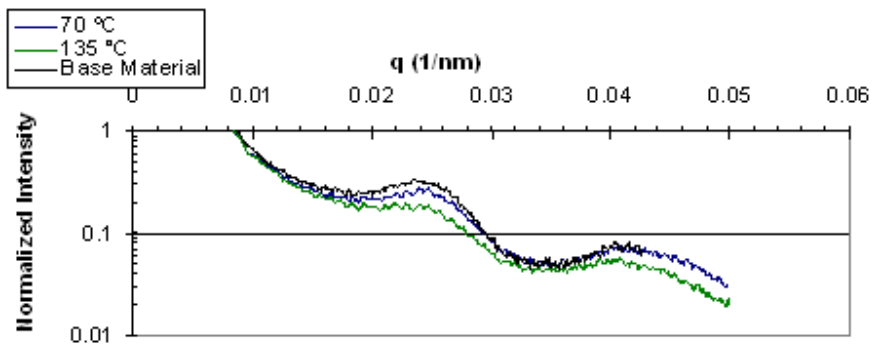


Figure 51: SAXD of C3 Samples

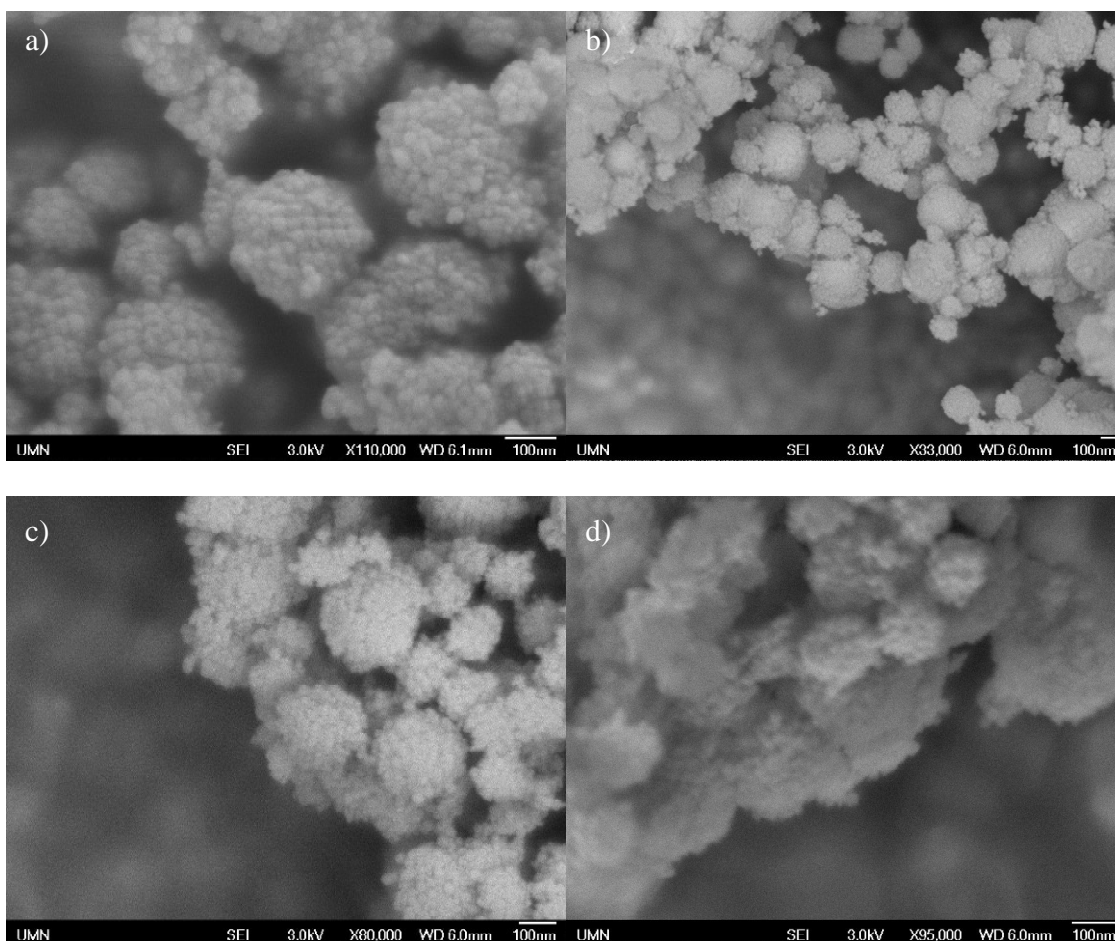


Figure 52: a and b at 135 °C and c and d at 70 °C

WAXD does not show any clear indication that the MFI structure is formed within the samples. SEM shows particles imprinted with the 3DOm structure. There does not seem to be any large MFI particles present in the sample or any significant changes to the 3DOm-i LTA. If MFI crystals were grown outside of the 3DOm-i LTA, one would expect large coffee shaped particles at 135 °C, while at 70 °C one would expect smooth round particles with a diameter of around 200 nm. Neither of which was observed in the SEM images from the two samples. Control images are represented below.

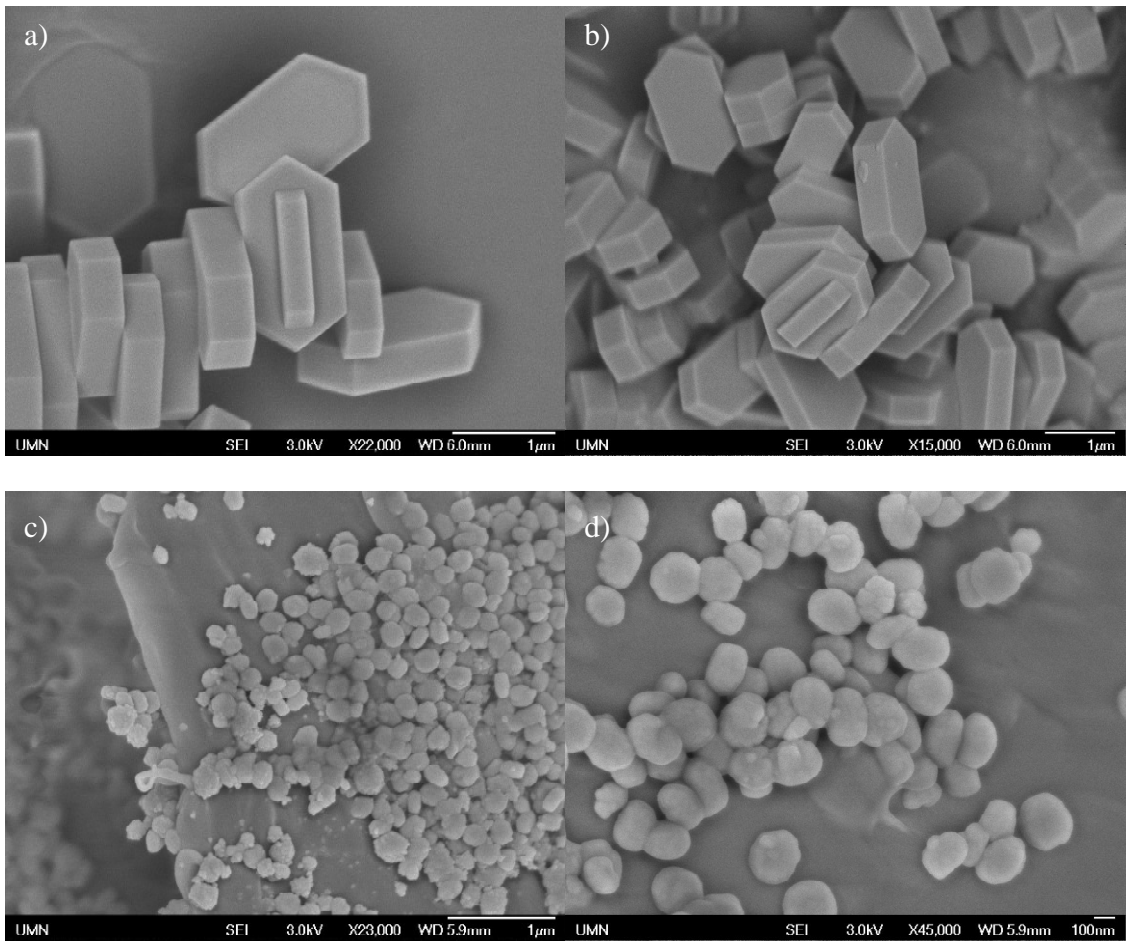


Figure 53: Control samples of C3 Solution: a and b from 135 °C and c and d from 70 °C

## Chapter 6

### Synthesis of 3DOm-i FAU zeolite

#### 6.1 Faujasite Structure

The Faujasite structure, commonly referred to as zeolite x and y, is an aluminosilicate zeolite composed of sodalite cages connected by double 6 member rings. This combination of secondary building blocks results in a cubic structure with 12 member rings along the [111] direction. The pore size of this structure is 7.4 Å. The chemical composition of faujasite unit is  $\text{Na}_x(\text{H}_2\text{O})_{240}\text{Al}_x\text{Si}_{192-x}\text{O}_{384}$ .

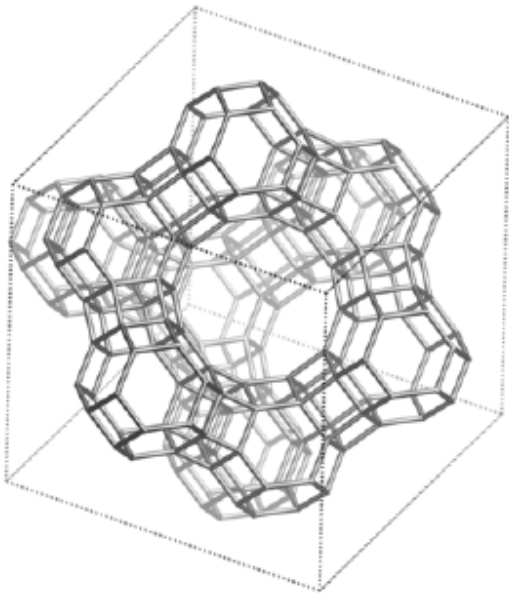


Figure 54: Faujasite framework viewed down the [111]<sup>20</sup>

Due to the similarity between the faujasite structure and the LTA structure, 6 double member ring versus a 4 double member ring, it stands to reason that FAU can be synthesized in a similar solution method of synthesis.

## 6.2 Initial Attempt at FAU synthesis in 40 nm 3DOm template

The first attempt to synthesize FAU particles within the 3DOm template using a solution method, similar to LTA, used a recipe previously shown to result in small FAU particles. The recipe used, reported by Li, utilized TMAOH as the structure directing agent.<sup>27</sup> A solution is generated by mixing 25 wt% tetramethylammonium hydroxide, 10 m NaOH, water, TEOS, and aluminum isopropoxide to generate the desired mole ratio of 2.46 TMA<sub>2</sub>O:0.032 Na<sub>2</sub>O:1 Al<sub>2</sub>O<sub>3</sub>:3.4 SiO<sub>2</sub>:370 H<sub>2</sub>O. The reagents were mixed in a plastic bottle overnight before filtering through a Whatman 542 filter. The clear solution was added to a Teflon liner containing 3DOm carbon, and then sealed in an autoclave. The reaction was performed at 130 °C for 3 days.

Following hydrothermal growth over three days, the solution becomes cloudy indicating the formation of zeolite particles in solution. The carbon was isolated from the growth solution and colloidal particles by filtration on a Whatman 542 filter. Water was used to wash the carbon removing any zeolite particles attached to the surface of the carbon. The carbon was then collected from on top of the filter pad and placed into a clean Teflon liner. Fresh growth solution was placed on the carbon, for an additional growth cycle. This process was repeated for 4 growth cycles.

During the carbon isolation phase, it was noticed that the cloudy solution did not readily pass through the filter. The carbon isolation became increasingly difficult with each growth cycle. For the fourth cycle, the product after hydrothermal growth was placed into a plastic bottle and additional water was added. After the carbon settled to the bottom, the top liquid, cloudy suspension of zeolite particles and unreacted material,

was removed with a transfer pipette. This was repeated 3 times before the carbon could be collected by filtration.

The use of four growth cycles produces a WAXD pattern of FAU; however the particle morphology does not suggest that growth was limited to the carbon template. Based on the difficulty in isolating the carbon template from the growth medium by filtration, it was expected that the particles produced by this recipe were large enough to get retained by the pores of the filter pad. Based on the successful LTA solution growth method, it can be extrapolated that a colloidal particle of approximately 130 nm in low yield can be successful for zeolite formation within the template.

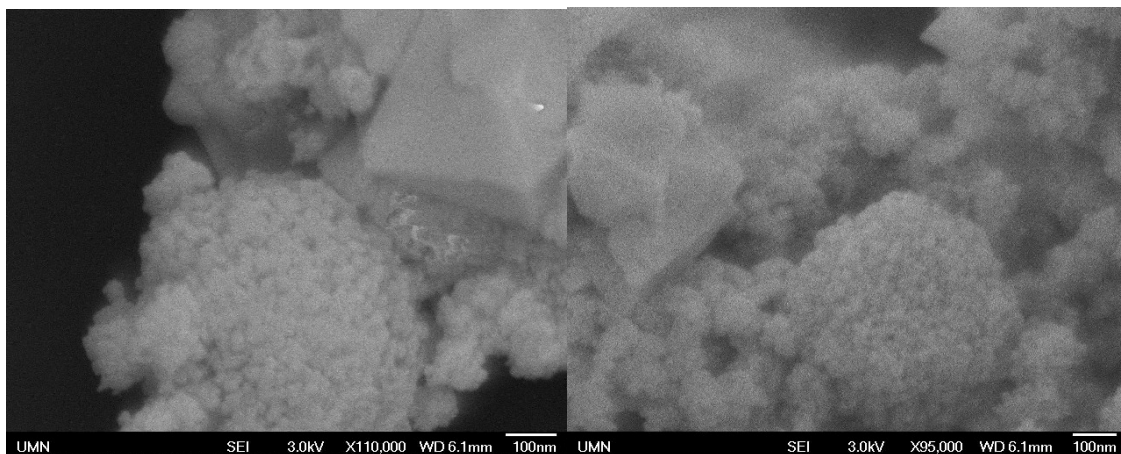


Figure 55: SEM images of 3DOm-i FAU synthesized along with FAU large crystals

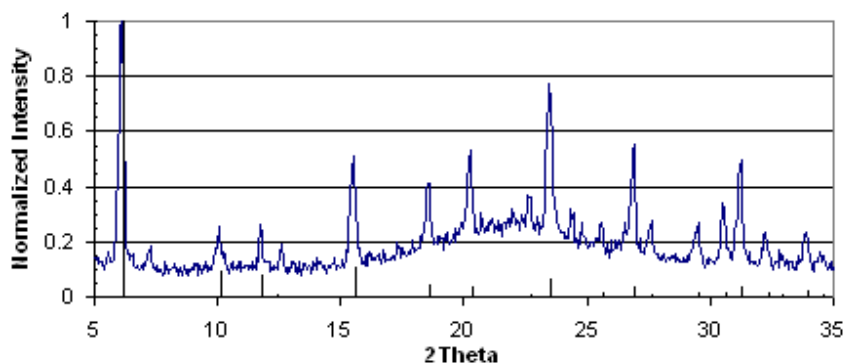


Figure 56: WAXD of 3DOm-i FAU

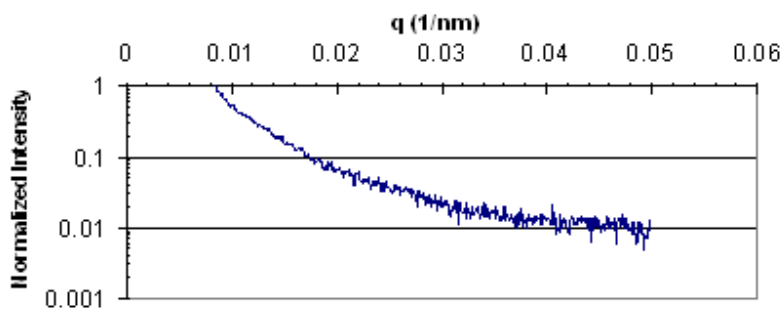


Figure 57: SAXD of 3DOm-i FAU

From the presented WAXD data from the sample, there are strong peaks located where one would expect diffraction from the FAU structure. There also appears to be weak peaks due to an impurity phase, LTA in the diffraction pattern. Using SEM, one can see that the 3DOm structure was imprinted upon some of the particles. There is, however, large crystal particles that were not imprinted with the desired 3DOm structure. From this data it is apparent that crystal growth outside of the template prevents the isolation of 3DOm-i FAU particles. This exterior crystal growth is also likely the source of the difficulty in filtration for carbon isolation as the crystal particles plug the pores of the filter pad. SAXD can be used to confirm what was observed with SEM. The SAXD

patturn does not show any diffraction peaks due to the mesoporous structure, which indicates that while some particles may have been imprinted with the desired structure they do not represent the majority of the sample and are not significant enough to result in strong diffraction peaks.

While these results are a promising starting point, the method used for 3DOM-i FAU needs to be further refined in order to prevent the formation of large particles on the surface of the carbon that cannot be easily removed by washing.

### 6.3 Alternative Recipe Directed at Templated Faujasite Synthesis

After this synthesis, the recipe used was altered to result in smaller colloidal particles that should be easily removed from the template by washing. Following a method similar to the one published by Wang<sup>28</sup> which is based off a colloidal FAU synthesis recipe published by Song<sup>29</sup>, preliminarily positive results can be obtained.

Tetramethylammonium hydroxide, 25 wt%, (TMAOH) is utilized as the structure directing agent. Aluminum is supplied from aluminum isopropoxide. The silica source is tetraethyl orthosilicate (TEOS). Sodium hydroxide and water are also used in the recipe. First TMAOH is measured into a vessel with a stir bar. Water and sodium hydroxide are then added to the TMAOH. Solid aluminum isopropoxide is then measured out and added to the bottle. The solution is mixed to dissolve the aluminum isopropoxide, sonication can be utilized to aid in the dissolution, which takes about one hour. After the aluminum isopropoxide is dissolved, the silica source (TEOS) is added dropwise to the solution. The solution is then mixed over night to age. The solution composition at this point has a mole ratio of 0.07 NaOH:2.4 TMAOH:0.5 Al<sub>2</sub>O<sub>3</sub>:2

SiO<sub>2</sub>:132 H<sub>2</sub>O. The solution is filtered through a 0.2 μm syringe filter before being added to the carbon. The solution is allowed to penetrate the carbon for 6 hours, before heating to 100 °C over 4 days for zeolite formation.

After 4 days, the autoclave is removed and cooled. The carbon is isolated from the growth media and zeolite particles grown outside of the carbon by filtering the sample over a Whatman 542 filter pad. Water is used to remove all the carbon from the liner and briefly wash the carbon. The washed carbon is then submitted to further growth cycles. Following completion of 3 growth cycle, the carbon was washed in warm water 5 times to remove any zeolite particles that may have adhered to the exterior of the carbon. During these wash cycles, the carbon is isolated from the wash water by vacuum filtration.

The growth by this method was followed by WAXD taken while the material was still in the carbon template. This allows for almost all of the material to be conserved, while gaining insight into how long it takes for crystallization to start to form within the template. In order to actually observe if the 3DOm structure is imparted on the zeolite, one needs to calcine the sample to observe it by SEM, TEM, and SAXD. This was performed after the 3<sup>rd</sup> cycle in order to get a better idea of the development of the material within the template.

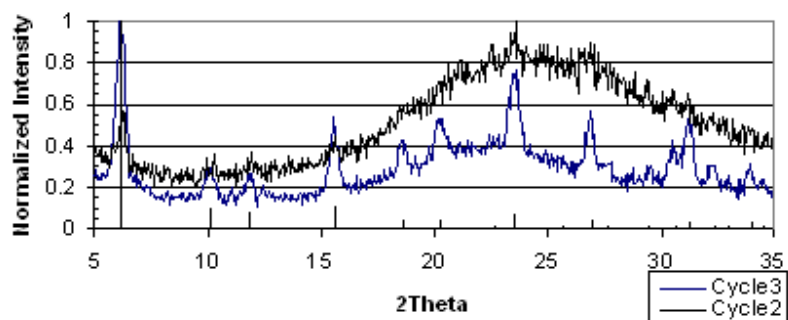


Figure 58: WAXD of Sample after Second and Third Cycles of Growth

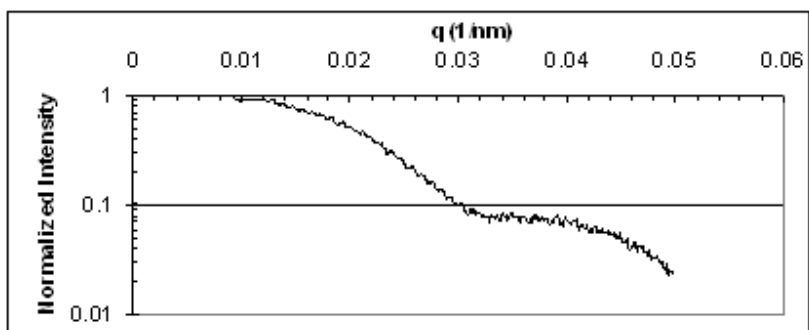


Figure 59: SAXD after Cycle 3 of Growth

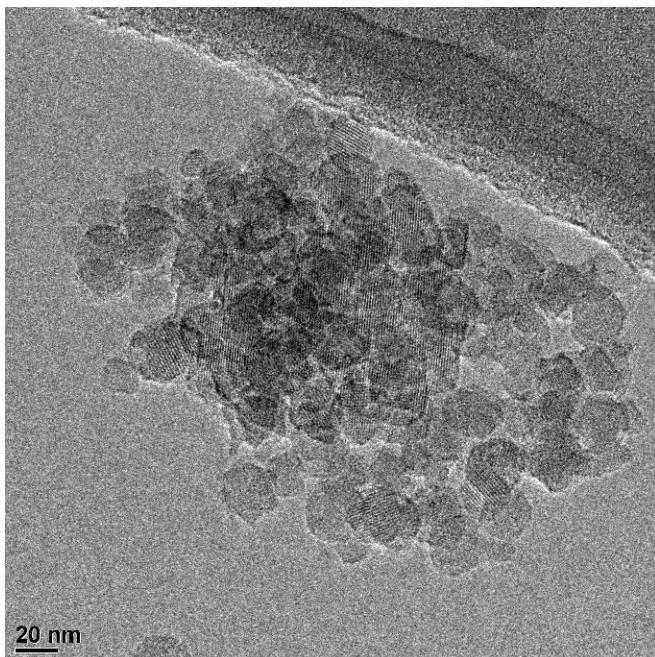


Figure 60: TEM Image of Material after Cycle 3 (Image by Xueyi)

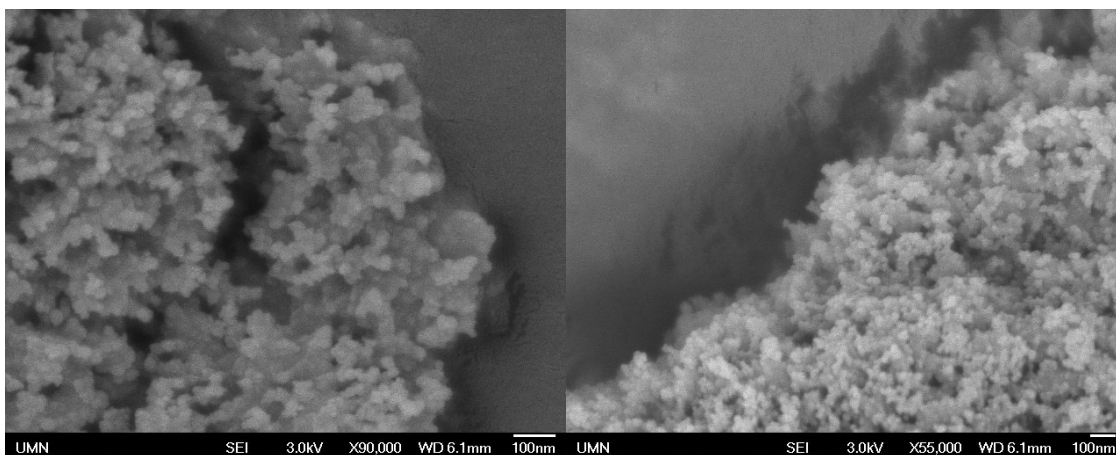


Figure 61: SEM Images of Material

The WAXD data shows the start of crystallization after cycle two, although the peaks are weak they are in the correct position expected for FAU. After cycle three there is significantly increased peak intensity. At this point it was considered worth investigating in greater detail. The sample was washed and calcined resulting in a very small yield of

product. The SEM shows the formation of small particles, which is expected based on the size of the template pores. The SEM does not demonstrate a clear formation of the template imprintation, however this may develop after further growth cycles. TEM data was also collected to prove that the particles formed are indeed crystalline, demonstrated by the lattice fringes displayed in the image. There are no SAXD peaks, which is expected based on the SEM. The mesoporous structure has not developed in this sample and is therefore not visible by diffraction.

This method needs further investigation to prove that the 3DOM structure can be formed, however this is a promising initial result that it should be possible to form 3DOM-i FAU.

An additional growth cycle was performed on the material within the carbon template to try and enhance the degree of ordering of 40 nm zeolite particles. By performing this additional growth cycle it is hoped to grow from the already present seed particles to form larger templated particles similar to what was observed with 3DOM-i LTA.

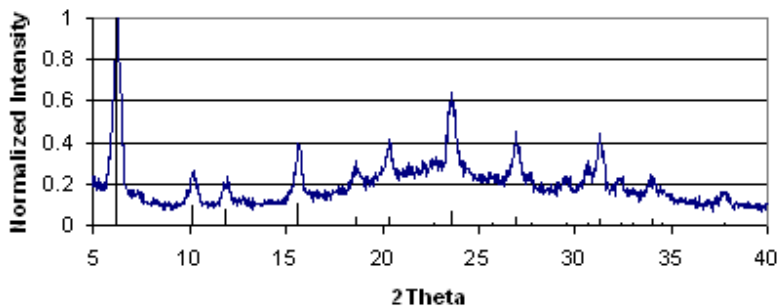


Figure 62: WAXD of Material after Calcination and 4 Growth Cycles

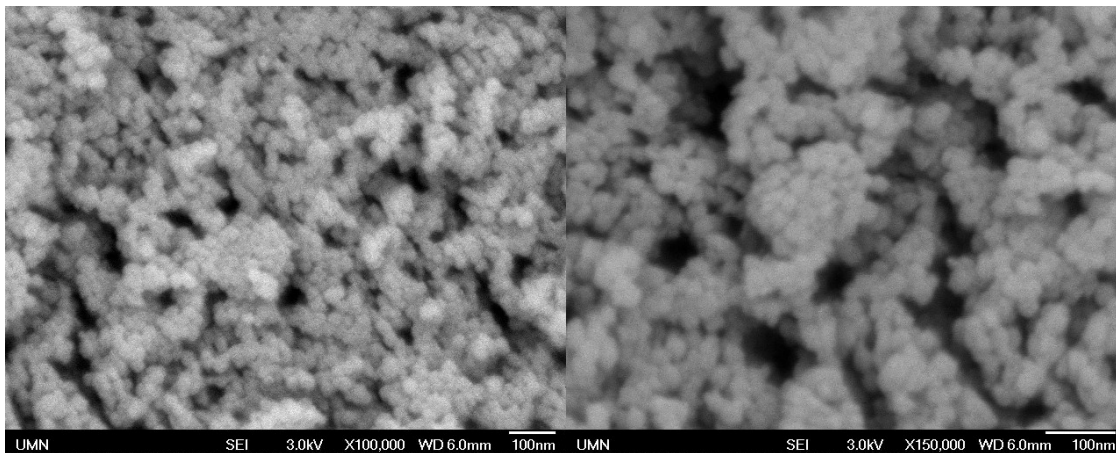


Figure 63: SEM Images of Material

From the SEM images it can be observed that a majority of the sample consists of 40 nm particles that have a relatively disordered packing, however there are some particles that seem to be the start of the formation of ordered packed templated particles. The particles can be confirmed to be the Faujasite phase by WAXD. This result proves the feasibility of synthesizing 3D*Om*-i FAU particles through the solution growth method.

#### 6.4 Characterization of Growth Suspension

As the previous chapter has indicated, the growth of 3D*Om*-i FAU feasibility, the colloidal suspension of growth media was characterized to gain insight into why these conditions lead the formation of Faujasite particles within the carbon template. From the solution with a ratio of 0.07 NaOH:2.4 TMAOH:0.5 Al<sub>2</sub>O<sub>3</sub>:2 SiO<sub>2</sub>:132 H<sub>2</sub>O, particles are formed within the template as well as remain in suspension. The suspension particles were washed with water until a near neutral pH was achieved. The particles were isolated from the solution through centrifugation of the particles. After reaching a near neutral pH the particles were characterized in suspension through dynamic light

scattering. Dynamic light scattering indicated a particle size of 190 nm with a high degree of mono-dispersity.

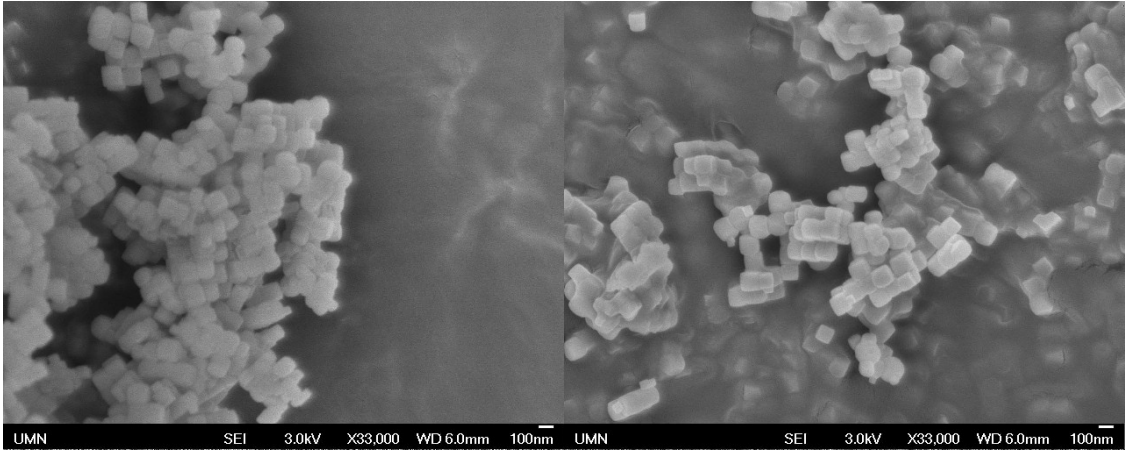


Figure 64: SEM Images of Colloidal Crystals from 3DOM-i FAU growth

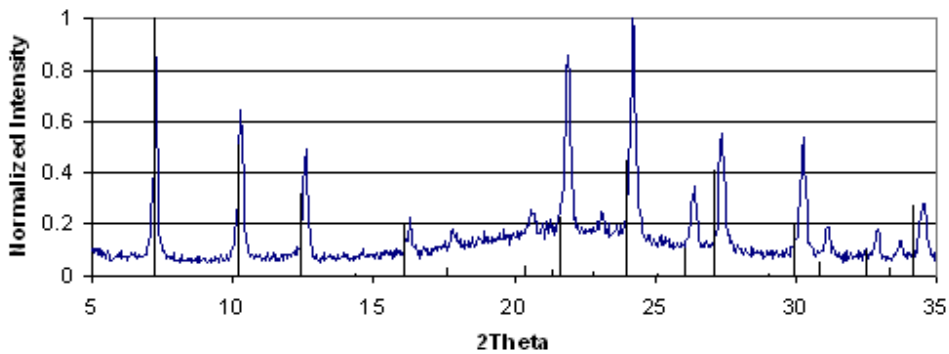


Figure 65: WAXD of Crystals from 3DOM-i FAU Growth with LTA Model Lines

Characterization of this suspension of particles show that the particles have a size around 200 nm and are highly mono-disperse in nature. The WAXD also determines the crystal phase to be LTA not faujasite. This is interesting since the particles in the carbon have the faujasite phase.

## Bibliography

1. Breck, D. W. Zeolite Molecular Sieves: Structure, Chemistry, and Use. John Wiley and Sons. 1974
2. S. Mintova, T. Bein. Nanosized Zeolite Films for Vapor-Sensing Applications. *Microporous and Mesoporous Materials*, 2001, 159-166.
3. Z. Wang, H. Wang, A. Mitra, L. Huang, Y. Yan. Pure-Silica Zeolite Low-k Dielectric Thin Films. *Adv. Mater.*, 2001, 746-749.
4. C. Platas-Iglesias, L. V. Elst, W. Zhou, R. N. Muller, C. F. G. C. Geraldes, T. Maschmeyer, J. A. Peters. Zeolite GdNaY Nanoparticles with Very High Relaxivity for Applications as Contrast Agents in Magnetic Resonance Imaging. *Chem. Eur. J.* 2002, 5121-5131.
5. N. Dubey, S. S. Rayalu, N. K. Labhsetwar, S. Devotta. Visible Light Active Zeolite-Based Photocatalysts for Hydrogen Evolution from Water. *International Journal of Hydrogen Energy*, 2008, 5958-5966.
6. M. E. Davis. Ordered porous materials for emerging applications. *Nature*, 2002, 813-821.
7. L. Tosheva, V. P. Valtchev. Nanozeolites: Synthesis, Crystallization Mechanism, and Applications. *Chem. Mater.*, 2005, 2494-2513
8. W. C. Yoo, S. Kumar, Z. Wang, N. S. Ergang, W. Fan, G. N. Karanikolos, A. V. McCormick, R. L. Penn, M. Tsapatsis, A. Stein. Nanoscale Reactor Engineering: Hydrothermal Synthesis of Uniform Zeolite Particles in Massively Parallel Reaction Chambers. *Angew. Chem. Int. Ed.*, 2008, 9096-9099
9. W. Fan, M. A. Snyder, S. Kumar, P. Lee, W. C. Yoo, A. V. McCormick, R. L. Penn, A. Stein, M. Tsapatsis. Hierarchical Nanofabrication of Microporous Crystals with Ordered Mesoporosity. *Nature Materials*, 2008, 984-991
10. S. Kim, J. Shah and T. J. Pinnavaia. Colloid-Imprinted Carbons as Templates for the Nanocasting synthesis of Mesoporous ZSM-5 Zeolite. *Chem. Mater.*, 2003, 1664-1668
11. V. N. Shetti, J. Kim, R. Srivastava, M. Choi, R. Ryoo. Assessment of the mesopore wall catalytic activities of MFI zeolite with mesoporous/microporous hierarchical structures. *J. Catalysis*, 2008, 296-303
12. Liu, Y. Zhang, W. T. J. Pinnavaia. Steam-Stable MSU-S Aluminosilicate Mesostructures Assembled from Zeolite ZSM-5 and Zeolite Beta Seeds. *Angew. Chem. Int. Ed.*, 2001, 1255-1258

13. M. Choi, H. S. Cho, R. Srivastava, C. Venkatesan, D. Choi, R. Ryoo. Amphiphilic organosilane-directed synthesis of crystalline zeolite with tunable mesoporosity. *Nature Materials*, 2006, 718-723
14. I. Schmidt, C. Madsen, C. J. H. Jacobsen. Confined Space Synthesis. A Novel Route to Nanosized Zeolites. *Inorg. Chem.*, 2000, 2279-2283
15. C. Jacobsen, C. Madsen, J. Houzvicka, I. Schmidt, A. Carlsson. Mesoporous Zeolite Single Crystals. *J. Am. Chem. Soc.*, 2000, 7116-7117
16. W. Xu, J. Dong, J. Li, J. Li, and F. Wu. A Novel Method for the Preparation of Zeolite ZSM-5. *J. Chem. Soc., Chem. Commun.*, 1990, 755-756
17. M. A. Snyder, J. A. Lee, T. M. Davis, L. E. Scriven, and M. Tspapatsis. Silica Nanoparticle Crystals and Ordered Coating Using Lys-Sil and a Novel Coating Device. *Langmuir* 2007, 23, 9924-9928
18. J. D. Rimer, D. G. Vlachos, and R. F. Lobo. Evolution of Self-Assembled Silica-Tetrapropylammonium Nanoparticles at Elevated Temperatures. *J. Phys. Chem. B*. 2005, 109, 12762-12771.
19. W. Stober, A. Fink, and E. Bohn. Controlled Growth of Monodisperse Silica Spheres in the Micron Size Range. *Journal of Colloidal and Interface Science*, 1968, 26, 62-69.
20. Ch. Baerlocher and L.B. McCusker, Database of Zeolite Structures: <http://www.iza-structure.org/databases/>
21. M. A. Snyder, M. Tsapatsis. Hierarchical Nanomanufacturing: from Shaped Zeolite Nanoparticles to High-Performance Separation Membranes. *Angewandte Chemie International Edition*, 2007, 46, 40, 7560-7573.
22. J. M. Newsam, M. M. J. Treacy, W. T. Koetsier, C. B. DeGruyther. Structural Characterization of Zeolite Beta. *Proc. R. Soc. Lond. A.*, 1988, 375-405.
23. Liu, Y. Zhang, W. T. J. Pinnavaia. Steam-Stable MSU-S Aluminosilicate Mesostructures Assembled from Zeolite ZSM-5 and Zeolite Beta Seeds. *Angew. Chem. Int. Ed.*, 2001, 1255-1258
24. I. Schmidt, C. Madsen, C. J. H. Jacobsen. Confined Space Synthesis. A Novel Route to Nanosized Zeolites. *Inorg. Chem.* 2000, 39, 2279-2283.
25. A. Sakthivel, A. Lida, K. Komura, Y. Sugi, K. V. R. Chary. Nanosized  $\beta$ -Zeolites with Tunable Particle Sizes: Synthesis by the Dry Gel Conversion (DGC) Method in the Presence of Surfactants, Characterization and Catalytic Properties.
26. T. M. Davis, T. O. Drews, H. Ramanan, C. He, J. Dong, H. Schnablegger, M. A. Katsoulakis, E. Kokkoli, A. V. McCormick, R. L. Penn, and M. Tspatsis. Mechanistic Principles of Nanoparticle evolution to Zeolite Crystals. *Nature Materials*, 2006, 5, 400-408.

27. Q. Li, D. Creaser, and J. Sterte. An Investigation of the Nucleation/Crystallization Kinetics of Nanosized Colloidal Faujasite Zeolites. *Chem. Mater.* 2002, 14, 1319-1324.
28. Z. Wang, M. A. Al-Daous, E. R. Kiesel, F. Li, and A. Stein. Design and Synthesis of 3D Ordered Macroporous ZrO<sub>2</sub>/Zeolite Nanocomposites. *Microporous and Mesoporous Materials*, 2009, 120, 351-358.
29. W. Song, V. H. Grassian, and S. C. Larsen. High Yield Method for Nanocrystalline Zeolite Synthesis. *Chem. Commun.*, 2005, 2951-2953.